

MULTIPHASE FLOW ESTIMATION USING DIGITAL IMAGE
PROCESSING

BY

ABUBAKAR, SHAMSUDEEN OLAWALE

A Thesis Presented to the
DEANSHIP OF GRADUATE STUDIES

KING FAHD UNIVERSITY OF PETROLEUM & MINERALS

DHAHRAN, SAUDI ARABIA

In Partial Fulfillment of the
Requirements for the Degree of

MASTER OF SCIENCE

In

SYSTEMS AND CONTROL ENGINEERING

MAY, 2016

KING FAHD UNIVERSITY OF PETROLEUM & MINERALS
DHAHRAN- 31261, SAUDI ARABIA
DEANSHIP OF GRADUATE STUDIES

This thesis, written by **Abubakar Shamsudeen Olawale** under the direction of his thesis advisor and approved by his thesis committee, has been presented and accepted by the Dean of Graduate Studies, in partial fulfillment of the requirements for the degree of **MASTER OF SCIENCE IN SYSTEMS & CONTROL ENGINEERING.**



Dr. Hesham K. Al-Fares
Department Chairman



Dr. Salam A. Zummo
Dean of Graduate Studies

29/6/16
Date

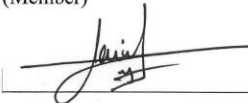




Dr. Moustafa Elshafei
(Advisor)



Dr. Sami El Ferik
(Member)



Dr. Mohamed A. Deriche
(Member)

© Abubakar, Shamsudeen Olawale

2016

ACKNOWLEDGMENTS

I am indebted to my thesis advisor, Professor Moustafa Elshafei for his inspiration, encouragement and overall supervision during this research work. His approachability and enthusiasm towards the research were particularly invaluable.

I am also grateful to my thesis committee members, Dr. Sami Elferik of Systems Engineering and Dr. Mohamed Deriche of Electrical Engineering. Their constructive criticisms and insightful suggestions were extremely useful.

I appreciate all members of the Faculty and Staff of the Department of Systems Engineering for their contributions in making my experience beneficial in many ways, as well as the inspiring camaraderie of my colleagues at the Department – Mahmoud, Jide, Dipo, Moustafa, Muideen, Najm, to name a few.

Finally, thank you to my family and friends, old and new, who supported me in varying ways throughout the course of my MSc. program.

TABLE OF CONTENTS

| | |
|--|------|
| ACKNOWLEDGMENTS..... | V |
| TABLE OF CONTENTS..... | VI |
| LIST OF TABLES..... | X |
| LIST OF FIGURES..... | XI |
| ABSTRACT..... | XIII |
| ملخص الرسالة..... | XIV |
| CHAPTER 1 INTRODUCTION..... | 1 |
| 1.1 Multiphase Flow Measurement Systems..... | 2 |
| 1.1.1 Comparison between MPFMs and other types of Multiphase measurement systems.... | 5 |
| 1.2 Multiphase Flow Meter (MPFM)..... | 7 |
| 1.2.1 Design of MPFMs: Operating Conditions and Accuracy Requirements. | 8 |
| 1.3 Methods used in MPFMs..... | 11 |
| 1.3.1 Volumetric Fraction measurement methods | 11 |
| 1.3.2 Component velocity measurement methods | 13 |
| 1.4 Some Commercially available MPFMs..... | 15 |

| | |
|--|-----------|
| 1.4.1 Safire 2.0..... | 15 |
| 1.4.2 Alpha VSR/VSRD | 17 |
| 1.5 Thesis Contributions..... | 18 |
| CHAPTER 2 BACKGROUND AND LITERATURE SURVEY | 20 |
| 2.1 Background..... | 21 |
| 2.1.1 Flow Visualization System (FVS)..... | 21 |
| 2.1.2 Processing Algorithms | 24 |
| 2.2 Literature Survey | 34 |
| CHAPTER 3 EXPERIMENTAL WORK..... | 39 |
| 3.1 Setup for flow experiments at RI..... | 39 |
| 3.1.1 Test section of the flow loop at RI..... | 40 |
| 3.1.2 Flow Vision System of the flow loop at RI | 41 |
| 3.1.3 Experiments | 42 |
| 3.2 Model experimental setup | 44 |
| 3.2.1 Test section of the model setup..... | 44 |
| 3.2.2 Flow vision system of the constructed model setup..... | 46 |
| CHAPTER 4 DEVELOPED PROGRAMS | 48 |

| | |
|---|-----------|
| 4.1 Conversion of Flow Videos to Frames..... | 49 |
| 4.2 Estimation of Liquid Holdup of Stratified flow..... | 49 |
| 4.3 Estimation of Wave Celerity of Stratified flow..... | 53 |
| 4.4 Estimation of Flow speed, Gas Volumetric Fraction & Average Gas speed of Bubbly flow | 56 |
| 4.4.1 Bubbly flow image preprocessing | 57 |
| 4.4.2 Estimation of properties of Bubbly flow from preprocessed images..... | 60 |
| CHAPTER 5 DISCUSSION OF RESULTS | 63 |
| 5.1 Liquid Holdup of Stratified flows | 63 |
| 5.2 Wave celerity of Stratified flows | 67 |
| 5.3 Gas Volume Fraction and Average Gas speed of Bubbly flows..... | 68 |
| 5.4 Flow speed of Bubbly flows | 71 |
| 5.5 Analysis of the developed programs | 73 |
| CHAPTER 6 RECOMMENDATIONS AND CONCLUSION..... | 76 |
| 6.1 Recommendations for future work..... | 76 |
| 6.2 Conclusion..... | 77 |
| REFERENCES..... | 79 |

VITAE.....87

LIST OF TABLES

| | |
|--|----|
| Table 3.1: Specifications of the Vision Research Speedsense 9040..... | 42 |
| Table 3.2: Fluid flow rates in experiments whose Stratified flows are studied..... | 43 |
| Table 3.3: Fluid flow rates in experiments whose Bubbly flows are studied..... | 43 |
| Table 5.1: Average run time of developed programs | 74 |

LIST OF FIGURES

| | |
|--|----|
| Figure 1.1: Using inferential methods used in a Three-phase (oil, water and gas) MPFM..... | 8 |
| Figure 1.2: Main flow regime types in horizontally inclined pipes (a) Bubbly flow (b) Stratified flow (c) Wavy flow (d) Plug flow (e) Semi-plug flow (f) Slug flow (g) Annular flow..... | 9 |
| Figure 1.3: Schematic of a Venturi meter..... | 14 |
| Figure 1.4: Safire 2.0 assembly and electronics | 15 |
| Figure 1.5: Weatherford Alpha VSRD installation on a test section..... | 17 |
| Figure 2.1: Some Preprocessing operations recommended for images of a bubbly multiphase flow | 29 |
| Figure 3.1: Schematic of experimental setup for flow simulations from which videos were obtained | 40 |
| Figure 3.2: Transparent portion of the test section; 22.5 mm ID..... | 41 |
| Figure 3.3: High Speed Camera used RI experiments, a Dantec Dynamics Speed Sense 9040..... | 41 |
| Figure 3.4: Pipe section of the constructed model test section..... | 45 |
| Figure 3.5: Basler ace acA2000-340kc Camera Link cameras..... | 46 |
| Figure 3.6: Hardware components of the flow vision system of the constructed model..... | 47 |
| Figure 4.1: Preprocessing of frames of stratified flow | 51 |

| | |
|--|----|
| Figure 4.2: Image of annular section with detected edges characterizing phase boundary..... | 52 |
| Figure 4.3: Flow image with labeling of liquid and gas areas respectively..... | 52 |
| Figure 4.4: Extracting flow wave..... | 54 |
| Figure 4.5: Plot of matrix of normalized cross correlation of $r_1(x, y)$ with $f_2(x, y)$ | 55 |
| Figure 4.6: $f_2(x, y)$ with the location of $r_1(x, y)$ as estimated by the program..... | 56 |
| Figure 4.7: A sample bubbly flow image taken by the camera in the FVS used in this work (Grayscale, 8bits/pixel, 1200 x 1632). | 57 |
| Figure 4.8: Bubbly image preprocessing. | 59 |
| Figure 4.9: Estimating average gas speed from processed bubbly flow images | 62 |
| Figure 5.1: Time series plot and distribution plots of estimated liquid holdup for 5 seconds of stratified flows..... | 65 |
| Figure 5.2: Time series plot of estimated wave celerity through frames for 5 seconds of stratified flows..... | 67 |
| Figure 5.3: Time series plots of estimated gas volume fraction and average gas speed for 5 seconds of bubbly flows | 70 |
| Figure 5.4: Time series plots of flow speed for 5 seconds of bubbly flows | 73 |

ABSTRACT

Full Name : ABUBAKAR, SHAMSUDEEN OLAWALE
Thesis Title : MULTIPHASE FLOW ESTIMATION USING DIGITAL IMAGE PROCESSING
Major Field : SYSTEMS AND CONTROL ENGINEERING
Date of Degree : MAY, 2016

Measurement of properties of multiphase flows is important because such flows are abundant in the process industry. Recent advancements in Digital image acquisition technology have made the use of digital image processing in multiphase flow measurement promising. This work contributes to the relatively few works that have explored this promise by developing Digital Image Processing programs that estimate properties of two-phase flows from images of experimental flows. Programs that estimate liquid holdup and wave celerity of Stratified flows as well Average Gas Speed, Gas Volume Fraction and Flow speed of Bubbly flows are developed using over 40,000 flow images obtained from experiments where two-phase stratified and bubbly flows in horizontal pipes were generated using air and water at superficial velocities between 0.1586m/s and 1.1583m/s. We also built a model test section with a potential to facilitate more extensive research. Trend plots of results from the developed programs show an agreement with known behavior of stratified and bubbly flows, indicating the practicability of the presented methodology.

Keywords: Multiphase flow measurement, Stratified flow, Bubbly flow, Digital Image processing

ملخص الرسالة

الاسم الكامل: شمس الدين أبو بكر اولوالي

عنوان الرسالة: تقدير معدل التدفق في وسط متعدد الأطوار باستخدام معالج الصورة الرقمي

التخصص: هندسة النظم والتحكم

تاريخ الدرجة العلمية: شعبان 1437

قياس خواص التدفق متعدد الأطوار أمر مهم لأن هذا النوع من التدفق متواجد بكثرة في العمليات الصناعية. التطورات الأخيرة في تكنولوجيا الحصول على الصورة والمعلومات جعل استخدام معالج الصورة الرقمي فعال وواعد في قياس التدفق متعدد الأطوار. هذا العمل البحثي مُكمل لبعض الأعمال القليلة التي اكتشفت هذه الطريقة بواسطة تطوير برامج معالجة الصورة الرقمي لتقدير خواص التدفق ثنائي الأطوار باستخدام صور تجارب تدفق عملية. البرامج المُستخدمة في تقدير حجم السائل و سرعة الموجه للتدفق متعدد الطبقات مثل متوسط سرعة الغاز بالبنز و الحجم الجزئي للغاز وسرعة التدفق في التدفقات الفقاعية قد تم تطويرها باستخدام أكثر من 40000 صورة للتدفق أخذت من تجارب عملية حيث قد تم توليد تدفقات متعددة الطبقات و فقاعية ثنائية الأطوار بانبوبة افقية باستخدام ماء وهواء حيث ان سرعة السطح تتراوح بين 0.1586 متر/ث و 1.1583 متر/ث. أيضا قد أعدنا نموذج اختباري مقطعي فعال لتسهيل العمل البحثي. النتائج المأخوذة من البرنامج المطور تظهر توافق سلوك التدفق مع تدفقات معروفة مسبقا لتدفقات متعددة الطبقات وبتدفقات فقاعية. هذه النتائج تشير الي مدي عملية الطريقة المقدمة.

CHAPTER 1

INTRODUCTION

Multiphase flow is a modeling generalization of flows containing fluids of two or more phases. Research in multiphase flows is essential in several applications such as the study of multiphase flows related to steam explosions is necessary in the design of industrial boilers and nuclear reactors. Two phase flows are of interest in pump cavitation problems, studies of climate systems such as clouds and groundwater [1]. Multiphase flow systems also arise many polymer processing operations. [2]

Flows in oil production wells typically consist of oil, gas and water from the reservoir, making three-phase flow in porous media a fundamental constituent of many oil recovery processes (e.g., gas injection, gas gravity drainage, surfactant flooding, and thermal recovery) [3] . These kinds of flows are even more prevalent in modern enhanced oil recovery methods, where water pumped into the reservoir eventually finds its way to the production well. [4]

Multiphase flow measurement is the metering of properties of constituent phases in a given multiphase flow. The demand for multiphase flow measurement is highest in the oil and gas industry because adequate knowledge of flow rates of individual components in producing oil wells is crucial in several operations in the industry, such as well testing,

production monitoring, production optimization, flow assurance, production allocation, and fiscal metering/custody transfer [5].

Although there has been significant research into multiphase flow, commercial multiphase flow meters are relatively new instruments and hence, a field where a lot of research is necessary. For example, dissimilarity between experimental and computational fluid dynamics (CFD) simulated results of these flow meters mean that there is a need to consider new approaches and obtain more data [5].

This work contributes to addressing this research problem by exploring the use of digital image processing techniques in developing multiphase measurement methods which are tested experimentally. In the rest of this chapter, we provide a backdrop to this research problem by introducing conventional designs and systems for multiphase flow measurement as well as some commercially available products. The objectives of this work and a summary of the organization of this thesis are also presented.

1.1 Multiphase Flow Measurement Systems

A flow meter is an instrument used primarily for measuring volumetric (or mass) flow rates of fluids typically while they are transported through a pipe. Flow meters for measurement of single phase (e.g. fuel pump meters) and those for multiphase flow (e.g. meters used at a wellhead) differ in the technologies they use and their complexity [6]

The processes used in multiphase flow metering systems can generally be grouped into four, namely, conditioning of the flow stream, volumetric component (or phase fraction)

measurement, component velocity (or phase velocity) measurements, and modeling of the multiphase flow. The combination of results from the volumetric component measurement and component velocity measurement is the means by which the volumetric flow rate is obtained. Phase density measurement process is included if mass flow rate is required [7].

Multiphase flow measurement systems can be classified based on these classes of processes. Using a classification suggested in [8], multiphase measurement systems can be categorized as:

i- Type I Multiphase Measurement Systems: This refers to conventional systems that use a combination of separators and single phase flow meters to achieve multiphase metering. The separator(s) split the flow into dedicated streams for its constituent fluids, the flow meters measure properties for each fluid, and the streams are then recombined to form the original stream.

These systems can be configured for continuous measurements but are typically used for intermittent or periodic measurement as test separators. Test separators arrangements are moderately accurate, with a typical flow rate accuracy of ± 5 to ± 10 % of each phase. Such intermittent use occurs in marginal fields developed across preexisting production platform, where economic or space constraints prevent the use of a dedicated separator [9].

ii- Type II Multiphase Measurement Systems: In systems of this type, a multiphase flow stream is divided into “gas rich” and “liquid rich” streams. Each stream is subjected to multiphase measurements and then recombined to form the original stream.

Differential Pressure meters (PD meters), Venturi for liquid phase velocity and Venturi/Vortex for gas phase velocity are typical techniques used for velocity measurement. Commonly used composition measurement methods include Dielectric analysis and gas/liquid split.

iii- **Type III Multiphase Measurement Systems:** Systems of this class offer simultaneous measurement of properties of multiple phases in a single meter, i.e. for a three phase flow; properties of all three phases are measured at the same time while the flow goes through a single conduit. Also referred to as Multiphase flow meters (MPFM) in literature, these meters are suitable for topside and subsea application and although uncertainty will be similar in either case, maintenance activities will be considerably more expensive in the latter [10].

These systems are relatively new and are gaining the most adoption in fields developed across preexisting production platforms, where economic or space constraints preclude the use of a dedicated separator. They are preferred to test separators with intermittent measurements and are installed in a growing number of minimal facilities [10].

‘Virtual’ Multiphase measurement solutions are also used in multiphase metering. In terms of modeling, there are three main types: empirical, which depends on the experimental data; mechanistic which is based on flow dynamical physics, but flow pattern dependent, and Homogenous models which assume homogenous flow characteristics [11]. They generally lack adequate traceability and are typically used as redundant systems to offer contingency measurements in the event of failure of main

meter employed. This may be a particularly important resource in subsea applications [10].

1.1.1 Comparison between MPFMs and other types of Multiphase measurement systems

i. Space and size: MPFMs are generally smaller than conventional separators and thus have less installation space requirement.

ii. Measurement Uncertainty: Considering different technologies and applications, current MPFM solutions generally have less accurate phase flow measurements than test separators, especially when MPFMs are used in cases where in-situ calibration of the device is not available. The main cause of increased uncertainties of MPFM measurements is that the flow meters in separator-flow meters methods deal with single phase flows which are less complex than multiphase flows [12].

iii. Data and Processing time: MPFMs have response times which are significantly lesser - minutes and even seconds - than that of separator-flow meter systems - hours.[12] and thus capable of providing much more relevant flow data in a given period.

iv. Versatility : Existing MPFM solutions are typically validated for a specific type of reservoir formation and using it for a different formation will require deployment of a different pipe diameter or materials to handle variations such as different gas and oil compositions or a greater presence of corrosive [5]. Separator-flow meter methods are generally more versatile in handling a range of reservoir formations.

v. Cost: Purchasing costs of MPFMs are generally higher than separator systems for a given multiphase flow measurement application. Subsea MPFM solutions, which is largest segment of the MPFM market, can range as high as \$1 million or more, but more typically fall between \$500,000 and \$750,000 [12]. Operating experience however suggests that overall lifetime costs of MPFMs can be considerably lesser in a variety of applications, due to reduced installation, operating, and maintenance costs.

Given these factors, conventional separator-flow meters method tend to be more suitable for operations where versatility and/or accuracy of the measurement system is of utmost importance, such as flow assurance, production allocation, and fiscal metering/custody transfer. MPFMs are more suitable for well characterization, development of subsea and remote satellite fields, and other applications where minimal installation space and/or large amount of data are most desired.

In practice, the choice of multiphase flow measurement method for a particular field is fundamental to the nature of the field development, with alternatives being to use MPFMs or separator-flowmeters systems alone or in combination. The economics of the field and the measurement standard that will be required are considered rather than 'fitting' a measurement approach to a particular field development. The optimal measurement solution is one where the need to maintain a low measurement uncertainty is balanced against the economics of the field development in question [10].

1.2 Multiphase Flow Meter (MPFM)

The primary information required in the measurement of oil and gas multiphase flow streams are the flow rates of oil, water, and gas. The ideal method to acquire this data would be to have a meter that would make such measurements directly. However, because of the properties of multiphase flows, such as slip between the liquid and gas phases, different possible flow regimes with overlapping features, and properties of the fluid, it is quite challenging to accurately obtain direct volumetric flow rate measurement of individual components without separating the flow into its constituent fluids [13].

MPFMs are flow meters that primarily measure volumetric flow rates of individual phases of a multiphase flow without separating the flow. They employ inferential techniques that use the cross sectional fraction and instantaneous velocity of each component, called phase fraction and phase velocity respectively, to make these measurements. If desired, mass flow rates of the components can also be evaluated using the densities of the components.

Figure 1.1 shows how flow metering is achieved by a 3-Phase MPFM for oil, water and gas in [9].

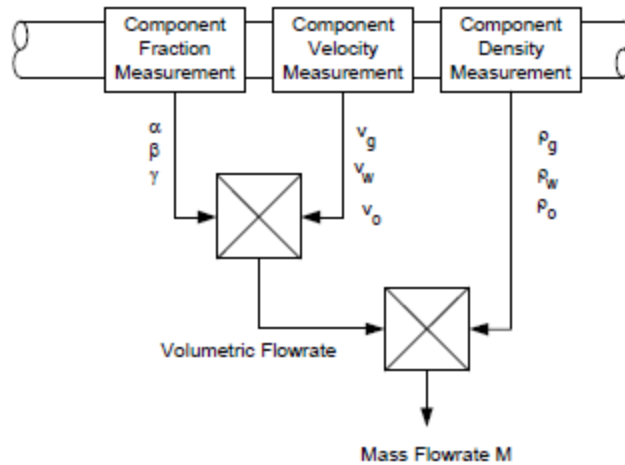


Figure 1.1: Using inferential methods used in a Three-phase (oil, water and gas) MPFM

Density information on the oil, water and gas phases is readily available by other methods. Oil, water and gas velocities – v_o , v_w and v_g respectively – and phase fractions– usually gas void fraction, α and water fraction, β – are the primary measurements of the MPFM and γ , the oil fraction is determined from

$$1 - (\alpha + \beta) = \gamma \quad (1.1)$$

1.2.1 Design of MPFMs: Operating Conditions and Accuracy Requirements.

The main design requirements of an MPFM are reliable measurement accuracy, ability to operate in harsh environments and requiring minimal human intervention. From their current use and applications where they are required in the oil and gas industry, MPFMs are expected to be able to measure oil, water and gas flow rates under a variety of conditions, such as

- i) 0% GVF (gas-void fraction) to 100% GVF,

- ii) 0% WLR (water in liquid rate) to 100% WLR,
- iii) Operating pressure condition up to 700 bar.
- iv) Temperatures up to 250°C.
- v) Over a wide range of flow speed (up to 30m/s) [13]

Variation in these parameters combined with pipe placement result in different types of flow profile [16]. Figure 1.2 below shows some of the main types of flow profiles that occur in horizontal pipes. Due to fluctuations in flow conditions in a typical multiphase flow, multiple flow profiles can occur over any length of time. A main flow profile, which is determined by the factors listed above, however occurs for longer periods and other flow profile(s) occur intermittently [1].

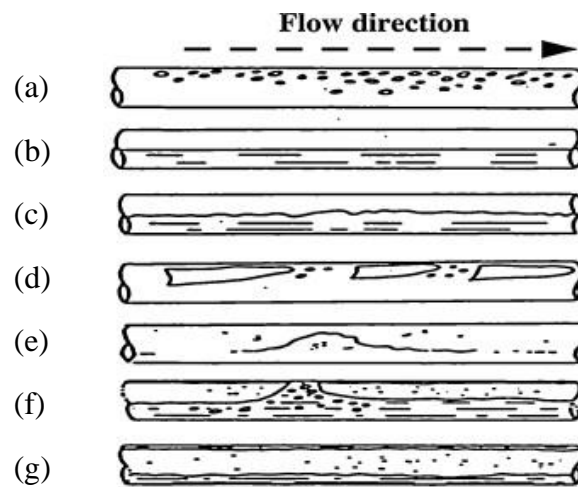


Figure 1.2: Main flow regime types in horizontally inclined pipes (a) Bubbly flow (b) Stratified flow (c) Wavy flow (d) Plug flow (e) Semi-plug flow (f) Slug flow (g) Annular flow

Downhole applications present some even more challenging requirements. In such applications, MPFMs are required to function at pressures up to 860 bar and temperatures

of 150 °C. In addition, the meter would be required to operate at any angle of orientation, and since it is not readily retrievable, it requires a mean time between failures (MTBF) of 5 to 10 years [9].

Absolute uncertainty ratings specify measurement accuracy in terms of percentage uncertainty associated with flow measurement of each phase. In the oil and gas industry, different uncertainty requirements are specified for different processes depending on the performance of available measurement technologies and the need to ensure proper reservoir management and long term sustainable production with maximum recovery [10].

A group of major oil companies reviewed their multiphase metering requirements and identified a common range of accuracy needs as:

- Relative error between total liquid flowrate and gas flow rate of 5 - 10% in flows with gas volume fraction 0 - 99% and a water cut range of 0 - 90%.
- absolute error in water cut measurement be less than 2% (Water cut is the ratio of water to the volume of total liquids in a multiphase fluid) [17]

Generally speaking, MPFMs are required to have a typical absolute measurement accuracy of $\pm 5\%$ of rate for each phase [18]. Advancements in production techniques and the exploitation of marginal fields are producing the need to meter over wider and wider component fraction ranges with fewer margins for measurement error.

The ideal MPFM will be non-intrusive, reliable, flow regime independent and suitable for use over the full component fraction range. Since inferential technique is used in MPFMs and a combination of measurements are required to determine flow rates, in order to

obtain uncertainties of less than 5%, individual measurements need to be obtained with much lower levels of uncertainty [9]. Factors that mainly affect the accuracy of measurements in MPFMs are properties of the measured fluid, flow regime properties and salinity characteristic of the flow and addressing these factors is a major area of current MPFM research.

1.3 Methods used in MPFMs

As earlier stated MPFMs use inferential techniques and provide flow information by estimating the volume fractions and the individual phase velocity of the components of the multiphase fluid. In this section, we describe some of the volumetric fraction and component velocities measurement methods.

1.3.1 Volumetric Fraction measurement methods

Volumetric fraction is also called phase fraction. Typical volumetric fraction measurement methods used in commercially available MPFMs can be divided into non-nuclear and nuclear methods.

The use of the nature of electrical properties of the multiphase flow is the major non-nuclear phase fraction measurement method in currently available MPFMs. The main principle of electrical impedance methods for component fraction measurement in MPFM is that the fluid flowing in the measurement section of the pipe is characterized as an electrical conductor. By measuring the electrical impedance across the pipe diameter (using contact or non-contact electrodes), properties of the fluid mixture like conductance

and capacitance can be determined. These properties are then related to phase fractions of the fluid (using methods such as look up tables) [12].

In MPFMs using nuclear method for phase fraction measurement, microwave or Gamma rays are used although the latter is more often used. The phenomenon that is leveraged upon in these methods is the attenuation of gamma rays passing through a multiphase flow.

Consider an MPFM with a gamma radiation source placed on one side of a pipe with internal diameter d , through which an oil, water, and gas mixture is flowing. The intensity of the beam after it has passed through the pipe is reduced relative to that of an empty pipe. If I_o is the intensity of the beam for the empty pipe, the intensity due to the mixture, I , is governed by the following relationship [8]:

$$I = I_o * C * \exp[-d (f_o u_o + f_w u_w + f_g u_g)] \quad (1.2)$$

where C is a constant related to the source and geometry of the set up and f_o ,

f_w , and f_g , are fractions of oil, water, and gas in the mixture. u_o , u_w , and u_g are the linear attenuation coefficient for the oil, water, and gas components.

In dual gamma ray method, two different gamma ray energy sources are used. Two independent equations which are similar to the above attenuation equation can be formulated. These two equations plus a third relationship, which is that the sum of volume fractions must equal to unity, can then be used to calculate the oil, water and gas fractions in a mixture using the dual gamma ray technique [8].

Gamma ray attenuation techniques for phase fraction measurement are non-intrusive and of lower cost than electrical impedance methods. Electrical impedance are however inherently safer as there are no radiation risks. Water salinity changes in the measured flow affect both methods for volume fraction determination [8] and thus have to be considered in the design of any MPFM.

The use of image processing techniques is a non-nuclear approach to phase fraction measurement that is currently being significantly researched due to its potential to provide a non-invasive and robust solution. Approaches include digital image processing [22] [23] [24] and tomography paradigms [9].

1.3.2 Component velocity measurement methods

Venturi metering and the cross-correlation are the most commonly used techniques for component/phase velocity measurements in MPFMs. Venturi metering is preferred for fluid velocity measurement of well mixed flows [19].

Venturi refers to a constriction in a pipe designed to give the venturi effect, which is a pressure drop when a liquid or gas flows through it. As fluid flows through a venturi, the expansion and compression of the fluids cause the pressure inside the venturi to change. In venture meters, the differential pressure across the upstream section and the throat section of the device is measured and can be related to the mass flow rate through the Venturi [12].

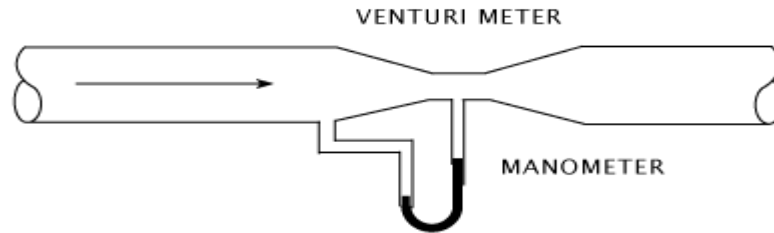


Figure 1.3: Schematic of a Venturi meter.

In MPFMs that obtain velocity measurement by cross-correlation, the variation in some property of the flow is measured by two identical sensors at two different locations separated by a known distance, L . As the flow passes the two sensors, a signal pattern measured at the upstream sensor will be repeated at the downstream sensor after a time dt , corresponding to the time it takes the flow to travel from the first to the second sensor. This time, dt , is obtained by a cross-correlating the signals from both sensors [12].

Technologies with which cross-correlation technique has been used/proposed for phase velocity measurements in MPFMs include:

- Gamma-ray (density) measurement
- Electrical impedance characterization
- Microwave measurement
- Differential pressure measurements
- Measurements using Image/Video processing methods

The accuracy of the cross-correlation technique depends on the validity of the assumptions used to in the functions that estimate the phase velocities from the dt obtained by cross-correlation and L [20]. In order to obtain accurate metering, designers must consider flow properties such a slip liquid and gas velocities.

1.4 Some Commercially available MPFMs

Over the last 25 years, significant research progress in MPFMs has led to the emergence of commercially available products. Developers have employed different technologies and modeling of the multiphase in designing MPFMs. This section presents an overview of two of the most recently developed commercially available MPFMs.

1.4.1 Safire 2.0

Jointly developed by and GE Measurement & Control, Los Alamos National Laboratory and Chevron ETC, Safire is noninvasive and provides real-time estimates of production flow rates from oil wells [13]. The device was first tested in 2008 and has been continually improved since then. Safire received the R&D Magazine's 52nd annual R&D 100 Awards in 2014.

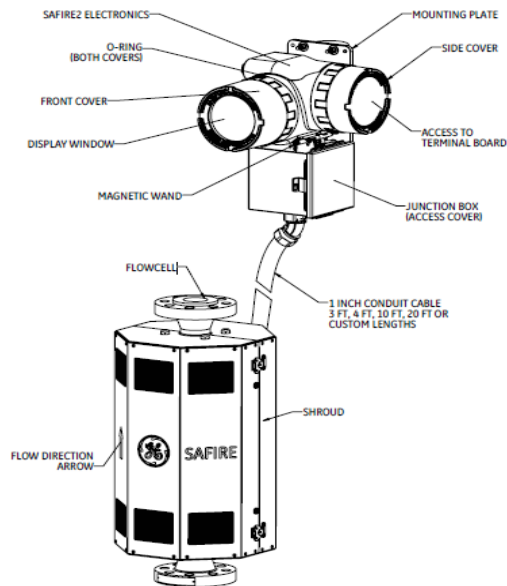


Figure 1.4: Safire 2.0 assembly and electronics [21]

Safire uses non-intrusive ultrasonic transducers, Correlation Transit-Time™ digital signal processing, LANL Swept Frequency Acoustic Interferometry (SFAI), Doppler, and wetted Microwave technologies [21]. SFAI uses (wideband ultrasonic) frequency-chirp through a multi-phase medium to extract frequency-dependent physical properties of said medium. The propagation time and the attenuation of the chirp signal as a function of frequency is then used to extract both fluid flow and multi-phase fluid composition information.

Some of the specifications of Safire models include [21]:

- Measure multiphase Flow with $\leq 40\%$ GVF and 0 to 100% WLR
- Typical uncertainty Water Cut measurement (absolute) $\leq 4\%$ and Liquid Rate (Relative) $\leq 5\%$
- Temperature Limits of : For Process/Fluid: 15 - 165°C (60 - 330°F). For Electronics: -40 °C to 60 °C (-40 °F to 140 °F)
- Can provide up to 100 readings/sec
- Hazardous Area Certifications • US/CAN: Cl. 1, Div. II, Gr. B, C & D – NEMA 4
• Global: ATEX/IECEX – II 3 G Ex nA IIB + H2 – IP 66
- Enclosure Material: Aluminum Si 12 High grade die cast • Weight: 17.64 lbs (8 kg) • Size (l x h x d): 13.2 in x 10.9 in x 8.5 in (33.5 x 27.7 x 21.6 cm) [not including junction box]

1.4.2 Alpha VSR/VSRD

Weatherford's Alpha VSRD (Venturi-nozzle Sonar Red Eye Densitometer) is based on a combination of an extended-throat Venturi meter, a sonar flowmeter, a Red Eye[®] MP water-cut meter and a gamma densitometer [7]. The Venturi meter and sonar flow meter, which uses an array of dynamic strain sensors to measure convection of turbulent vortices, are used to overall flow velocity measurements.



Figure 1.5: Weatherford Alpha VSRD installation on a test section

The gamma densitometer uses a small radioactive source, Caesium-137, and measures the radiation attenuation across the process pipe to get phase fraction estimates. The Red Eye[®] MP water-cut meter is a filter spectrometer that employs the principle of near-infrared absorption to measure water content in a liquid or multiphase stream [7].

Features of the VSRD include [7]:

- Measure multiphase Flow with 0% to 98% GVF and 0 to 100% WLR
- Temperature Limits of (i) Process/Fluid: -20 °C to 85 °C; (ii) Electronics: -40 °C to 70 °C. Pressure rating : 206.84 bar

- Typical absolute uncertainty Water cut /Liquid flow rate $\leq 10\%$ and Gas flow rate $\leq 5\%$. Repeatability of measurements : +/- 0.1% to +/- 3%
- 11 to 30 VDC supply voltage, < 30W
- RS485 serial port with 6'' color touchscreen
- Hazardous rating : Class 1, Division 1
- Material : 316/316L stainless steel

Alpha VS and Alpha VSR are other flow meters by Weatherford for wet gas fixed or variable water cut.

1.5 Thesis Contributions

This work contributes to efforts aimed exploring the use of digital image processing techniques in developing usable multiphase flow measurement methods. Our particular contributions include:

- Implementing a model multiphase flow vision system consisting of a flow imaging system, pipe section and a PC on which images are displayed and processed.
- Developing image processing programs for estimation of properties of stratified and bubbly flows.
- Testing and analyzing the developed programs with on-line images of two-phase stratified and bubbly flows.

The rest of this thesis is organized as follows: Chapter 2 presents a background of digital image processing techniques and paradigms that are useful in this work and a survey of works in literature with similar objectives to this work. Chapter 3 describes the experimental efforts in this work including the experiments from which test images were obtained and the model flow vision system that was developed. Chapter 4 explains the programs developed for this work and chapter 5 presents a discussion of results obtained using those programs on images obtained from experiments. Conclusions that were inferred and recommendations for future work are presented in Chapter 6.

CHAPTER 2

BACKGROUND AND LITERATURE SURVEY

One of the most prominent issues with current MPFMs is that they require frequent re-tuning because they lack robustness against flow regimes changes [22]. A major reason for this lack of robustness is their need to identify the flow regime first for better estimation of the other multiphase flow parameters. Flow regimes are more than 20 types including bubble flow, slug flow, annular flow and many more, and they depend on many factors such as pipe inclination, phase composition and physical properties, and velocity of the individual fluids [23]. The overlapping between these flow regimes, especially at the transient zones makes the identification rather difficult and misidentification introduces metering errors, as these meters usually assume one type of flow regimes and are tuned based on it. Thus, improved identification of the correct flow regime at different time interval will greatly improve the multiphase flow measurement [24].

A promising approach to addressing this challenge is the utilization of Computer vision in designing MPFMs, where intelligent algorithms based on Image processing techniques are used to identify multiphase flow properties such as hold up, bubble size distribution, bubble length and slug frequency. These estimated properties are in turn used for identification of flow regimes changes and estimation of phase fractions and velocities.

The advancement of video processing systems and availability of low cost recording system and powerful computing system enabled the use of Image processing in MPFM design [25], [26]. The major objective of this work is to research the use of video and

image processing paradigms in multiphase measurement by testing developed programs on videos of flow from experiments.

In this chapter, we provide a background on system and methods that are used in Image processing MPFMs as well as a review of works that are related to using Image processing in multiphase flow. The chapter is organized as follows: Section 1 provides a background of Image processing MPFM system and methods that have been mentioned in different works of literature. Section 2 presents a survey of some works in literature whose objectives are related to the objectives of this work.

2.1 Background

A flow visualization system and image processing algorithms are the major constituent parts of MPFMs that are based on Image processing.

2.1.1 Flow Visualization System (FVS)

Flow visualization system consists of three main components: Imaging system, Illumination system and processing unit [26]. The Imaging system is usually a high speed video capturing device such as high speed camera. The specifications of the high speed camera should be carefully selected based on the objective and application.

The first specification to be considered is the camera's frame rate which is defined as number of frames per unit time (usually in seconds; FPS) or the camera's frequency (Hz). This specification should be chosen based on a general sense of the range of velocity to

be recorded so that the camera captures necessary details of the flow with little redundancy [27]. Generally, as the flow velocity increases, FPS should also increase, and its value may be as low as 60 FPS and high up to 10000 FPS [28]. The type of intended application – offline or online - is another factor that affects the FPS specification. In online applications, FPS should be minimized in order to reduce the processing time.

Shutter speed or exposure time, usually expressed in fractions of a second, is the amount of time each frame is exposed to light and is another important specification of a FVS. This feature should be carefully tuned to get clear images and avoid getting blurred images [27]. Applications for high velocity flows require a fast shutter speed that is optimized for freezing the fast moving objects in the frames while avoiding redundant frames.

A third important specification is image spatial resolution which is defined as number of pixels or dots per unit area. Spatial resolution should not be confused with pixel resolution, which is the total number of count of pixels in the image which gives the dimension of the image. Spatial resolution rating of the camera determines the clarity of the acquired images. It depends on properties of the imaging system and is in effect, the number of individual pixel values per unit length, typically measured in pixels per inch (ppi) in camera images. Although high spatial resolution is preferred to show flow details more clearly, this results in longer recording time and fewer frames per second. Therefore, there should be a compromise between image spatial resolution and frame rate [29].

The second component of the FVS is the illumination system. There are several illumination devices that can be used to illuminate the flow such as light emitting diode array [29], fluorescent lamp, Halogen lamp [30], etc. Laser is preferred for contaminated liquid [25]. The choice and arrangement of the illumination system for the test section in the flow loop is done in order to avoid light reflection and have a uniform illumination so as to eliminate the need for advanced preprocessing of acquired image. Techniques that have been suggested to improve the quality of the illumination include installation of a rectangular transparent box filled with water around the test section pipe to reduce the image distortion from light source [25], setting up a diffusive surface between the lamp and box [27] or using diffusive light emitting diode array to achieve uniform illumination [29]. Using reflected light on white screen to illuminate the test section is another technique that has been suggested to improve the quality of the acquired image of the flow [30].

A unit for processing the image processing based algorithms of the MPFM is the third component of the FVS. It is usually a PC with high computing power and fast processing speed that is appropriate for requirements of the intended application. For an intended application, online processing generally requires faster and more powerful processing units than offline processing. The camera is connected with the PC through one of several interfaces including USB, Firewire, Gigabit Ethernet (GigE). Required Cable length, immunity to industrial noise due to electromagnetic fields and speed of data transfer are some of the factors that determine proper interface selection [30].

2.1.2 Processing Algorithms

Algorithms used in research related to Image processing for MPFM related can be grouped into Image processing algorithms and computational intelligence algorithms. Image processing algorithms can further be divided into Image preprocessing algorithms and algorithms for estimation of multiphase flow parameters such as holdup, bubble size, etc. Computational intelligence paradigms have also been used to improve flow feature estimation from images and to evaluate properties of the flow such as type of flow regime, flow velocity. In this section, we briefly discuss the most widely used approaches in these algorithm classes.

A. Image preprocessing Algorithms

The complex nature of multiphase flows makes the preprocessing of multiphase flow images a very essential part of design of MPFMs using image processing in order to enhance the quality of the image to be processed and improve accuracy of the estimations. There are various preprocessing methods and appropriate techniques are selected based on flow environment and vision system used. Common image preprocessing steps include:

- i. **Image color conversion:** These are used to convert color images, usually in the RGB (Red, Green, and Blue) color system, to gray image. Widely used approaches include finding the average of the most prominent and least prominent colors or averaging all three colors. A generally more accurate method is Luminosity. In this approach, weights that are optimized for clarity are assigned to each color [31].

ii. **Contrast Enhancement:** This is necessary in order to improve the identification of boundaries between liquid and gas phases. Two main methods for contrast enhancement are:

a. Histogram equalization: Here, image contrast is improved by adjusting image intensity using the normalized histogram of the image. Let f be the input image and g be output image. The normalized histogram of f , p_n , is:

$$p_n = \frac{\text{number of pixel with gray level } n}{\text{total number of pixels}}; \quad n = 0, 1, \dots, L-1 \quad (2.1)$$

L is the number of possible intensity level, which is 256 for a gray image.

The histogram equalized image, g , is then given by:

$$g_{i,j} = \text{floor} \left((L-1) \sum_{n=0}^f p_n \right) \quad (2.2)$$

Contrast-limited Adaptive Histogram Equalization (CLAHE) is a histogram equalization contrast enhancement method which operates on small regions rather than entire image [31].

b. Contrast stretching: In this approach, a *linear* scaling function is applied to the input image pixel values.

$$p_{out} = (p_{in} - c) \left(\frac{b-a}{c-d} \right) + a \quad (2.3)$$

a is the lower limit intensity value for the image type ($a = 0$ for gray image) and b is the upper limit intensity value for the image type ($b = 255$ for gray image). c and d are lower and upper limit of pixel values in the current image while p_{in} is the pixel value before stretching and p_{out} is the pixel value after stretching.

Contrast stretching is simpler than the histogram equalization method and results in an enhancement that is more pleasant [32].

iii. **Illumination Correction:** This preprocessing operation is done to address non-uniform illumination in the acquired image. The process is based on background subtraction, where a homogenous background with objects that are darker or brighter than the background is assumed [33]. Two main methods in illumination correction algorithms are Prospective correction and Retrospective correction.

In prospective correction, several images are simultaneously captured with the primary input image. The additional input images can be dark (background with no light) or bright (background with light but not objects) and are used to obtain the illumination corrected image. If bright and dark images are available, the corrected image can be obtained by:

$$NC = \text{mean}(f(x, y)) \times \frac{1}{\text{mean}\left(\frac{f(x, y) - d(x, y)}{b(x, y) - d(x, y)}\right)}$$

$$g(x, y) = \frac{f(x, y) - d(x, y)}{b(x, y) - d(x, y)} \times NC \quad (2.4)$$

(x, y) is the image spatial coordinate system, $f(x, y)$ is image with non-uniform illumination and $g(x, y)$ is the processed image. $d(x, y)$ is dark image, $b(x, y)$ is bright image, and NC is normalization constant.

Retrospective correction methods are used when only one input image is available. It works by estimating the background and subtracting it from a bright input image. One implementation of this method is to perform Low pass Filtering (LPF) of the image with a large kernel in order to estimate its background. The illumination-corrected image is then obtained as:

$$g(x, y) = f(x, y) - LPF(f(x, y)) + mean(LPFF(f(x, y))) \quad (2.5)$$

iv. **Conversion to binary image:** In order to label objects in the multiphase flow images as belonging to liquid or gas phases, it is necessary to convert the acquired image into a binary image using a threshold that is defined for the classification of the image objects. Approaches to Image thresholding that are suitable for images two phase flow include Global Thresholding and Adaptive thresholding.

In Global thresholding methods, the thresholding function is defined for the entire image and may be a simple binary function or based on statistical properties of the entire image. The Otsu technique is a global thresholding technique that calculates an optimal threshold to use in converting a grayscale image to a binary image by assuming the grayscale image has a bimodal histogram and maximizing the interclass variance of the modes [31].

Adaptive Thresholding methods divide the image into sections, usually rectangular areas or on a pixel by pixel basis and a thresholding function is defined for processing the

sections. Amount of noise and relative size between background and image objects are factors that are considered in defining regions. Adaptive thresholding methods are better than Global thresholding methods in handling noisy images. They are iterative and thus generally take longer processing time [31].

For classification of objects of Multiphase flows images into more than two classes, multi-level or color thresholding approaches are used. They include RGB thresholding, Hue Saturation Value (HSV) and Hue Saturation Luminance (HSL) thresholding methods.

v. **Image restoration:** This is the removal of noise from the acquired image. Image restoration methods include filtering, such as the use of a low pass filter to smoothen the image and median filter to remove salt and pepper noise. Gaussian filter based are efficient for removing high frequency noise and lossless image compression. [31]. Image restoration algorithms based on Iterative statistical algorithms such as Lucy-Richardson and computational intelligence paradigms [35], [36], [37] are more suitable for complex image restoration tasks like the Blind image deconvolution problem.

vi. **Morphological operations:** These are nonlinear mathematical operations used to enhance the image and extract image features. Dilation and Erosion are the two basic morphological operations. Dilation allows the object to expand and is useful for objectives like filling small holes and connecting disjoint objects. Erosion is used to shrink objects by eroding their boundaries.

Dilation and Erosion can be combined into more complex operations such as opening and closing. Opening, which is erosion followed by dilation, enables the removal of unwanted

small objects while closing, which is dilation followed erosion, facilitate filling small holes and gaps. These operations are essential for identifying flow features such as bubble size and shape [31], [34].

vii. **Image Resize:** Resizing images to be processed can be useful in reducing processing time. The minimum bounding box algorithm is the most widely method for cropping desired sections of images [28]. Generally, the algorithm finds an oriented enclosing box for a set of points that is smallest in terms of perimeter, area or volume. For a set of points in a 2-D plane, like an image, a minimum-area or minimum-perimeter enclosing rectangle linear time algorithm that is used.

The fewer the amount of preprocessing operations required for images acquired by the imaging system in the FVS, the lesser the overall processing time in MPFMs using Image Processing. In order to require fewer / less complex preprocessing operations, it is important to use a FVS with optimal specifications in the imaging and illumination systems. Figure 2.1 shows some of the preprocessing operations suggested in [15] for a bubbly flow.

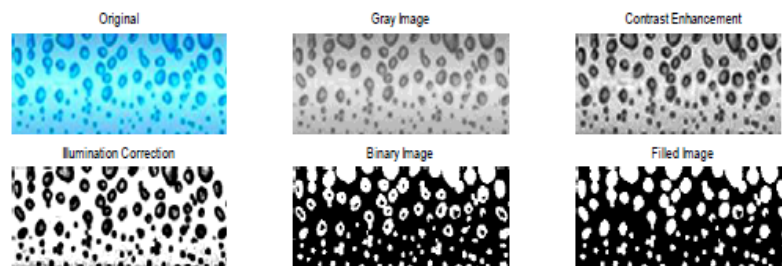


Figure 2.1: Some Preprocessing operations recommended for images of a bubbly multiphase flow

The complex nature of multiphase flows, non-uniform illumination of the captured flow and imperfections in the imaging system necessitate the use of some (or all, depending on the intended estimation and quality of the images) of the preprocessing operations described above in any system for multiphase flow measurement using Digital image processing.

B. Algorithms for flow Feature estimation

In MPFMs using Image processing, properties of Multiphase flow such as flow regime type and phase and flow velocities are evaluated from features of the flow such as holdup and bubble characteristics, which are estimated using objects in acquired (and preprocessed) images. This section gives a brief review of some methods used for estimation of holdup, fluid velocity and bubble characteristics.

i. **Holdup:** Holdup is the fraction of a particular fluid in a pipe interval. Due to gravitational forces and other factors, each fluid in a multiphase flow moves at a different speed, with the lighter phase travelling faster, i.e. being less held up, than the heavier phase [39]. Holdup is a key parameter in estimation of properties of multiphase flow.

To estimate Holdup in MPFMs using Image processing, the area of each phase in flow image are labeled. Depending on flow condition, two main approaches are used in Image processing holdup estimation algorithms:

a) **Labeling by using boundary:** In this approach, edge detection techniques as canny operator or morphological boundary extraction algorithms are used to

identify phase boundaries [28]. The algorithms are suitable for flow regime types with clear boundaries, such as stratified flow and plug flow.

b) Labeling using the pixel intensity: This method is used for flow regimes with unclear phase boundaries such as wavy, annular, and dispersed annular flows. In these flow types, three phases can be present- gas, liquid, and mixed phase – and this makes it difficult to clearly identify boundaries between different phases. The variety of pixel intensities in the mixed phase due to non-uniform mixing also makes the identification more difficult. A general approach for this method is to classify the pixels of the gray image into six different levels based on the intensity values [28].

After labeling the liquid and gas phase objects in the image, their holdup can be calculated as:

$$h_l = \frac{A_l}{A} ; \quad h_g = 1 - h_l \quad (2.6)$$

where h_l is liquid holdup, A_l is area of image occupied by liquid phase image objects and h_g is gas holdup.

For an estimation that is robust to flow regime changes, using a combination of the methods yields the best results. For three phase flows, the use of a combination of both algorithms is necessary as just labeling phase boundaries is insufficient for holdup estimation. Volume, instead of cross sectional area, has also been used in estimating volumetric hold up [40].

ii. **Fluid Velocity:** Approaches used for Image processing algorithms for fluid velocity estimation include Bubble Tracking and Cross correlation. In bubble tracking, bubbles are identified by assigning a label to the center of the mass of each bubble. The displacement of a bubble's center of mass in the time interval between successive frames in which it appears is then used to estimate bubble (and by extension, fluid) velocity [29]. The method is inefficient for flows with large number of bubbles or large number of bubble coalescence and break-up events, and thus cannot be used for turbulent flows.

Cross correlation is used to estimate fluid velocity by evaluating the displacement of some flow property, such as bubbles and waves. Flow image cross correlation is a promising technique for fluid velocity estimation in multiphase flow. Image cross correlation is primarily performed in two and three spatial dimensions and between successive frames, and is different from time varying signal cross correlation that is used in conventional flow meters.

A cross correlation function, $R_{x_n y_n}()$, in [27] for tracking the displacement of Taylor bubbles over M frames is given by :

$$R_{x_n y_n}(pTr) = \frac{Tr}{M} \sum_{c=0}^{M-1} x_I(c) y_I(c+p) \quad (2.7)$$

p is the shift in the number of frames and Tr is the frame rate resolution. M is the number of images used to calculate the cross correlation and I is the pixel spatial index. $x_I(c)$ and $y_I(c+p)$ are the intensity values associated with pixel I in the c^{th} and $(c+p)^{th}$ images respectively.

Using the cross-correlation, the length of the bubble can be estimated as the pixel distance between the peak and zero of the cross-correlation signal.

A more sophisticated cross correlation approach is presented in [15] to estimate displacement in the direction of flow. In the work, the cross correlation between a template t and an image f is gotten as:

$$R(u, v) = \frac{\sum_{x,y} [f(x-u, y-v) - \bar{f}_{uv}] [t(x, y) - \bar{t}]}{\sqrt{\sum_{x,y} [f(x-u, y-v) - \bar{f}_{uv}]^2 \sum_{x,y} [t(x, y) - \bar{t}]^2}} \quad (2.8)$$

\bar{f} is the mean value of f under the template, t , and \bar{t} is the mean value of the template. u and v are the offset between the images.

The procedure returns a matrix R of the values of the correlation, from which the offset (u^*, v^*) in pixels correspond to the peak of the correlation. A similar cross correlation function is developed for 3-D objects.

The velocity of the phase whose object is cross correlated can then be obtained from:

$$U(t) = \beta \frac{d(t)}{W} FOV / t_{fr} \quad (2.9)$$

$d(t)$ is the displacement in pixels between frame at time t and frame at time $t-1$, W is the image width in pixels and FOV is the field of view (i.e. width of the image of the pipe) in meters. β is the frame period, which is a calibration correction value to compensate for variability in FOV .

iii. **Bubble Size:** Bubble parameters are important features for estimating flow type. The general approach for bubble size analysis algorithms is to assume a shape for the bubbles, usually spherical or ellipsoid, and project the bubble on a 2D plane. Spherical bubbles are projected as circles and then the radius of the bubble can be estimated. Assuming a spherical bubble shape however reduces the bubble size distribution accuracy because non-circular bubbles are not analyzed [29].

2.2 Literature Survey

Measurement of properties of multiphase flow provides information that is necessary for the design and optimal operation of flow systems. Experimental techniques and methods that have seen significant usage in the research of multiphase flow include capacitance sensor [43], wire-mesh sensor [44], constant electric current method (CECM) [45], ultrasonic detection technique [46], impedance method [47], X-ray tomography [48], gamma-densitometry [49], Laser focus displacement meter [50] and Laser Doppler Anemometry [51].

In recent years, optical measurement techniques have been gaining increased usage in the development and application of methods for multiphase flow studies. These include Particle Tracking Velocimetry (PTV), Particle Image Velocimetry (PIV), Shadowgraphy, and Digital image processing. One example of such work is the combined application of PTV and PIV to determine bubble sizes and velocities as well as the liquid velocity field in a bubbly. Single or multiple exposure images of the flow seeded with tracer particles,

which are illuminated with light from a pulsed laser, are used in the study to obtain images that are processed to track bubbles in order to obtain bubble properties [29].

In [10] and [11], Shadowgraphy and PIV were used in image processing algorithms for a simultaneous evaluation of the velocity fields of the continuous phase and the dispersed phase in a circular water column with bubbly flow. In [54], the bubble size and velocity were evaluated using imaging and shadowgraph methods. Two black-and-white CCD cameras in stereo configuration were used to obtain particle images which were analyzed using algorithms that can correctly estimate the size of spherical and of non-spherical particles.

Artificial intelligence techniques have also found application in such experimental research, especially for flow pattern classification and holdup estimation. Artificial Neural Network (ANN), with 7 inputs based measured pressure values, were used for the classification of flow regimes of a three phase flow in a vertical pipe in [52]. In [53], Adaptive Neuro Fuzzy Interference System (ANFIS) was used for classification of 4 flow regimes – Stratified smooth, Stratified Wavy, Annular and Slug. The designed system had 5 inputs, including pressure and temperature measurements, and gave good classification results except in transition zones due to overlapping of flow regimes. In [42], the pre-processing of input data to an ANN for flow regime identification was studied. Simulation results on an ANN that uses two inputs to identify 4 types of multiphase flow was used to conclude that by using natural logarithm normalized and scaled inputs, improved flow identification can be achieved in transition regions.

A benefit of advances in digital video acquisition and processing systems in recent years is that high quality videos of fluid flow can be recorded. This has advanced multiphase flow research by facilitating works on visualization of transportation process in multiphase flow [55], modeling of solid particles mixed in gas-fluid flow for fluid dynamics problems [56], and several fluid mechanics applications [57] [58]. Due to the ubiquitous nature of multiphase flows in the oil industry in particular and process industries in general, these advances have made the use of Digital image processing methods in multiphase flow properties measurement research a contemporary research area with huge promise [42][64]. Compared with other experimental techniques such as PTV, use of sensors, etc., using DIP in multiphase flow measurement offers a means of achieving a higher level of detail about the flows and as such has a great potential to facilitate highly accurate studies of flow properties such as bubble trajectory and interaction [29]. The non-intrusive nature of these techniques make them suitable for studying flow regimes sensitive to disturbances, such as plug, slug and annular flows. A necessity for optical access to the flow can be seen as the only demerit of using digital image acquisition and processing methods in flow research.

In works that use digital image processing for multiphase flow measurement, flow videos are generally converted into individual frames, which are then processed to extract desired flow parameters for different flow regimes. The characterization of motion in a bubble column using imaging techniques was introduced by [59] [65]. However, the work only achieved a general characterization of the flow and no methods were developed to track individual bubbles (or transparent objects) until [54]. Using stroboscopic background illumination and stereo imaging, they developed a method for

tracking and sizing spherical glass beads dispersed in water. They showed that stereo imaging diminishes depth of field distortion but efficiency of bubble tracking is reduced by uneven light distribution [66].

In [60], high-speed cinematography and image analysis techniques were used to develop bubble recognition and tracking algorithms for measuring bubble size, velocity, interfacial area and coalescence behaviour in a 2D bubble column. The results of the work showed a high fluctuation in bubble size measurement and bubble velocity measurements owing to size range of generated bubbles - 10 to 25 mm -, superimposition of bubbles and significant surface tension. By using an LED array to illuminate the recorded flow in a similar setup and for similar measurements, [29] improved the illumination thereby achieving better bubble recognition and tracking. However, bubble clusters (touching bubbles) were difficult to distinguish from ellipsoidal bubbles. An attempt to solve this problem was presented in [61] [67] by using a method based on high-speed cinematography and matching recorded flow patterns to manually selected templates but could only achieve a marginal reduction of the effect of overlapping bubbles, bubble clustering and uneven illumination.

Back-illuminated flow images from a high speed digital camera were used in [62] [68] to study the bubbles in slug and plug flows. In acquiring the flow video, an automatic adaptive adjustment of time delays is used to synchronize each bubble passage with frame acquisitions. The method achieves real time estimation of individual bubble velocity, allowing for the capture and characterization of multiple bubbles (that are within the camera field of view and) travelling at different velocities, a scenario common in plug and slug flows in horizontal pipes.

The implementation of digital image processing technique to study the stratified two-phase flow is scarce [52] [63]. The pressure gradient and holdup characteristics of a dispersion-free stratified wavy flow of oil-water fluid in horizontal and slightly inclined were studied using images from a high speed video camera in [52][69]. Contact angle in the flow were obtained by processing flow images and used in developing a simple equation for estimating the interface shape based on the constant-curvature-arc model. Favorable comparison of the model's predictions with data from literature is reported as suggesting a potential for practical application. The researchers in [63] estimated the interfacial wave characteristics of different air-water stratified flows in a horizontal pipe. Visualization images from flows of 24 couples of superficial air and water velocities were characterized into four types of stratified flows based on their liquid holdup distribution that was estimated using flow image processing.

CHAPTER 3

EXPERIMENTAL WORK

The developmental work in this thesis is based on videos from experiments performed in the Research Institute (RI) of King Fahd University of Petroleum and Minerals. In order to potentially facilitate further research and the feasibility of deploying the system, a model test section was also constructed.

3.1 Setup for flow experiments at RI.

The setup for flow experiments at RI whose schematic is shown in Figure 3.1 is capable of handling two liquid phases and one gas phase. The main components include one tank and pump for each liquid, a test section, two separation tanks that are attached at the end of the test section, a return pump close to the separation tanks, and an air compressor. The tanks have an inner diameter of 1.25 m and height of 1.6 m. The pumps have a power rating of 3.5 HP and can pump liquid to a maximum velocity of 3 m/s.

The liquid lines are joined to the test section via a Y-shaped mixing section. While most of the flow test section is made of PVC pipes, a part located towards the end of the section is made of a transparent Plexiglas. In the experiments used for this work, the multiphase flow consisted of air and water at velocities between 0.1586 m/s and 1.1583 m/s.

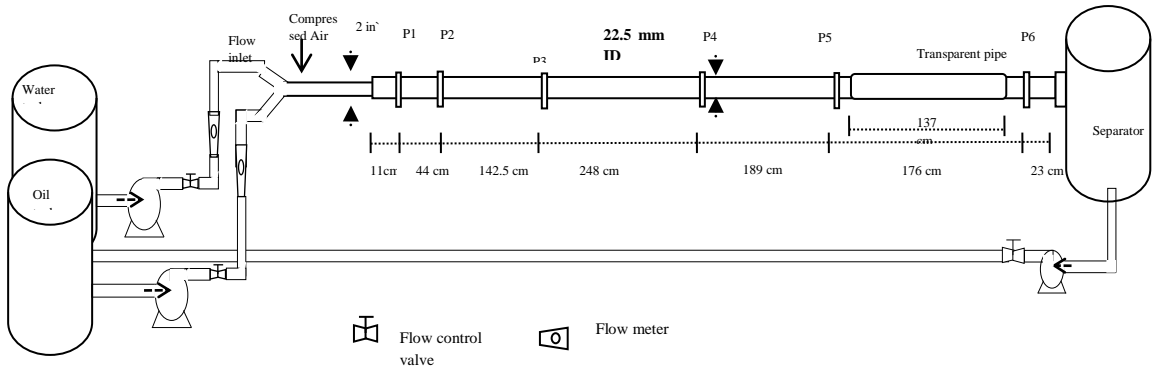


Figure 3.1: Schematic of experimental setup for flow simulations from which videos were obtained

3.1.1 Test section of the flow loop at RI

It consists of pipes with an inner diameter of 22.5 mm and with the exception of the portion of the section that is for visualization, the pipe is made of PVC with ASTM D-1785 standard number.

The pipes are installed horizontally. The total length of the test section is 8 m. The portion of the test section that is made of PVC pipes is suitable for pressure measurements and the rest of the section is made of Plexiglas, making it transparent and suitable for visual observation of the flow. Differential pressure transducers and manometers are attached along outlets that are distributed along the pipe for pressure measurement. The transparent portion of the test section is shown in Figure 3.2.



Figure 3.2: Transparent portion of the test section; 22.5 mm ID.

3.1.2 Flow Vision System of the flow loop at RI

The camera that is part of the flow vision system in the experimental setup is a Vision Research SpeedSense 900xx high speed camera. It is part of a vision acquisition system for industrial application that is produced by Dantec Dynamics. The system also includes the DynamicStudio software for image acquisition.



Figure 3.3: High Speed Camera used RI experiments, a Dantec Dynamics SpeedSense 9040

Principal specifications of the camera are shown in Table 3.1. The image resolution and video frame rate can be adjusted by the user. In choosing the settings, the objective is to use settings that adequately capture the required flow details from flow but are not higher

than necessary in order to keep space required for video storage and time required for video processing reasonable.

Table 3.1: Specifications of the Vision Research Speedsense 9040

| Model | Maximum Resolution (Pixels) | Bit Depth | Maximum Exposure Time (μ s) | FPS | Pixel Size (micron) |
|-------|--------------------------------|-----------|-------------------------------------|-----------|------------------------|
| 9040 | 1632 \times 1200 | 8 ,12 ,14 | 2 | 1016 /508 | 11.5 |

For the experiments whose flow images are used in this work, the principal camera settings used were:

- Image resolution: 1280 \times 720 pixel.
- Video frame rate: 1000 FPS.

3.1.3 Experiments

Experiments that result in stratified and bubbly flows of an air-water fluid were conducted for this work. Because of the many interactions going on in a given multiphase flow, what is common is to have a flow regime interrupted by another kind of flow regime from time to time. For the experiment for which stratified flows videos were recorded, the flow rate of gas was within 0.0001136m³/s (1.8gpm) and 0.0001325m³/s (2.1gpm) while the flow rate of the liquid was between 0.0001312m³/s (2.08gpm) and 0.0001319m³/s (2.09gpm). Similarly for the second set of the experiments from which

videos of bubbly flows are recorded, the gas flow rate was between 0.0001262m³/s (2.0gpm) and 0.0004416m³/s (7.0gpm) and the liquid flow rate was between 0.0001199m³/s (1.9gpm) and 0.0001388m³/s (2.2gpm). Superficial velocities of both fluids that correspond to flow rates in the experiments that were performed are shown in Table 3.2 and Table 3.3. These velocities are estimated from:

$$V_{Sl} = \frac{Q_l}{A_p} ; V_{Sg} = \frac{Q_g}{A_p} \quad (3.1)$$

where Q_l and Q_g are liquid and gas flow rates respectively and A_p is the cross sectional area of the pipe (with pipe ID = 22.5mm; $A_p = 0.0003976\text{m}^2$). V_{Sl} and V_{Sg} are liquid and gas superficial velocities.

Table 3.2: Fluid flow rates in experiments whose Stratified flows are studied

| Case No | Gas Flow Rate (m ³ /s) | Liquid Flow Rate (m ³ /s) | V _{Sg} (m/s) | V _{Sl} (m/s) |
|---------|-----------------------------------|--------------------------------------|-----------------------|-----------------------|
| 1 | 0.0001136 | 0.0001312 | 0.2875 | 0.3300 |
| 2 | 0.0001199 | 0.0001319 | 0.3016 | 0.3317 |
| 3 | 0.0001262 | 0.0001312 | 0.3173 | 0.3300 |
| 4 | 0.0001325 | 0.0001319 | 0.3332 | 0.3317 |

Table 3.3: Fluid flow rates in experiments whose Bubbly flows are studied

| Case No | Gas Flow Rate (m ³ /s) | Liquid Flow Rate (m ³ /s) | V _{Sg} (m/s) | V _{Sl} (m/s) |
|---------|-----------------------------------|--------------------------------------|-----------------------|-----------------------|
| 1 | 0.0001262 | 0.0001199 | 0.3173 | 0.3316 |
| 2 | 0.0001451 | 0.0001325 | 0.3649 | 0.3332 |
| 3 | 0.0003344 | 0.0001199 | 0.8410 | 0.3316 |
| 4 | 0.0004416 | 0.0001325 | 1.1106 | 0.3332 |

3.2 Model experimental setup

As shown in Table 3.2 and Table 3.3, only a limited number of experiments could be generated with the setup described in Section 3.1. In an attempt to facilitate further research into the use of image processing in multiphase flow measurement of stratified and bubbly flows, one of the objectives of this work was to construct a model test section that allow such flows to be generated with an online estimation of their properties. This section describes the test section that was built towards achieving that objective.

The constructed model test section can be used to generate flows of a mixture of air and water. Its main components include two tanks, a pipe section, one water inlet pump, and a compressed air supply. The pump has a power rating of 0.37 KW and a maximum discharge rate of 20 l/min at 220V. The pipe section is made of PVC pipes.

Visualization of the flow in the test section is done using an imaging system that consists of two cameras, two frame grabbers, a PC controller and relevant softwares. Lighting for the cameras is provided using LEDs that are mounted at a point in the body of the pipe section such that the emitted light is generally perpendicular to the flow and camera lens. Transparent acrylic sheets are used to protect the camera lens from direct contact with the flow.

3.2.1 Test section of the model setup

The pipe section of the assembled model experimental setup is shown in Figure 3.4. One-way ball valves are used to control fluid flow. Flow meters and manometer are also

installed along the length of the pipe section. The pipes have an inner diameter of 25.4 mm and are made of PVC with ASTM D-1785 standard number.

The pipes are installed horizontally. The total length of the test section is 1.85 m. Two points along the length of the pipe section are set up as joints to allow the installation of one camera at each point. The first point is located 0.73m after the mixing point of the water and air supplies, and the second point 0.61 m after it. Holes are made at the side of the fittings used to make these joints to facilitate the installation of LEDs to light up the recorded flow.



Figure 3.4: Pipe section of the constructed model test section

3.2.2 Flow vision system of the constructed model setup

Two Basler Ace acA2000-340kc Camera Link cameras, shown in Figure 3.5, and associated hardware and software necessary for flow video acquisition are the components of the imaging system in the constructed model experiment.



Figure 3.5: Basler ace acA2000-340kc Camera Link cameras

The cameras have CMOS sensors and a maximum image resolution of 2048 x 1086. They have a camera link interface and are rated to deliver 340 frames per second at 2 MP resolution. Their pixel bit depth can be set to 8, 10 or 12 pixels. 16mm, 25mm and 35mm Computar lenses were available for the prototype construction and those with a focal length of 16 mm and focal ratio 2.0 were found to be of suitable use for the test section.

The cameras are connected to a National Instruments (NI) PXIe (PCI eXtensions for Instrumentation) 1435 image acquisition modules through PoCL Camera Link SDR/MDR cables. Each of the frame grabbers are installed in one slot of the 4-slot NI PXIe-1071 3U PXIe Chassis. The Chassis also carries the NI PXIe-8135 controller, which is a 2.3GHz, Core i7 processing unit with Windows 7 installed. A 17-inch monitor, keyboard and mouse are connected to the controller.



Figure 3.6: Hardware components of the flow vision system of the constructed model.

Pylon CL Configurator software was used to configure the port settings of the cameras. Flow videos were obtained with the video acquisition tool of MATLAB R2013b and camera files that were created using NI Camera File generator.

CHAPTER 4

DEVELOPED PROGRAMS

When two fluids simultaneously flow in horizontal pipes, several flow patterns can form. At very low superficial velocities of the individual fluids, the flow is stratified with a more or less smooth boundary between layers of the individual fluids. Interfacial waves occur when the flow rates increase and such flow configuration is generally referred to as Stratified wavy. With a further increase in superficial velocities, the flow pattern becomes dual continuous, with both phases retaining their continuity at the top and the bottom of the pipe as they were in the stratified flow, but with a dispersion of one phase into the other along the waves [1]. With an increase of superficial velocity, there is a formation of structures of gas contained in liquid (generally called bubbles) of different possible sizes, resulting in different possible flow regimes. One such regime is the Bubbly flow where small to moderately sized bubbles are discretely diffused or suspended in a liquid continuum.

Studying the properties of stratified multiphase flow regime is important for understanding the transition from the stratified to the dual continuous pattern and for predicting pressure drop along the flow. [1] . Properties of bubbly flows of wet gas - such as gas volume fraction, average gas speed, etc. - in natural gas production change depending on reservoir conditions; and in order to ensure an efficient use of production resources, it is essential to estimate these properties.

In the rest of this chapter, developed image processing programs that are used to study characteristics of stratified flows and bubbly flows are described. The programs are developed using flow videos obtained from the experimental setup described in the previous chapter. The experiments were performed as part of research for a PhD dissertation [64] [68]. All programs are implemented using MATLAB R2015b.

4.1 Conversion of Flow Videos to Frames

In all the programs, the first step was to convert the recorded flow videos to individual frames. As it is common in literature, in the rest of this chapter, “frame” and “image” are used interchangeably. The MATLAB Videoreader object and some associated functions were used to carry out the conversion and storage on disk. With a consideration for speed of conversion and storage requirement, a comparison of available video recording formats and image formats to which extracted frames could be stored in was carried out and AVI format was selected for video recording and frames were saved as JPEGs. The video was recorded in grayscale to reduce the processing time by not needing a conversion from another color space to grayscale.

4.2 Estimation of Liquid Holdup of Stratified flow

Holdup is the fraction of a particular fluid in a pipe interval. Due to gravitational forces and other factors, each fluid in a multiphase flow moves at a different speed, with the lighter phase travelling faster, i.e. being less held up, than the heavier phase [39]. Holdup

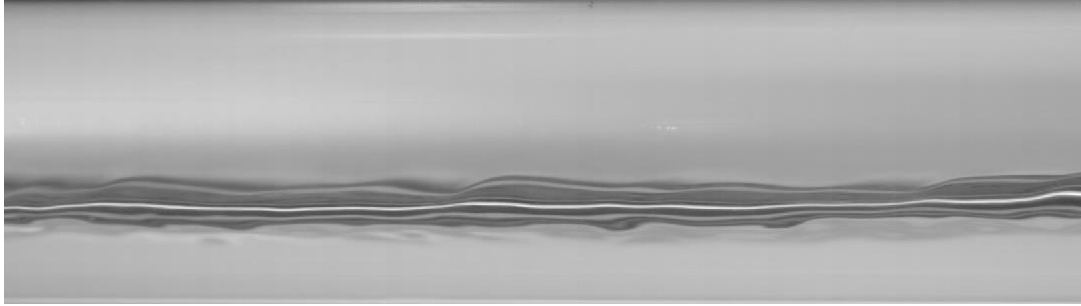
is also called in-situ volume fraction and due to its importance in multiphase equipment/process design, it is a key parameter in multiphase flow measurement. For example, accurate predictions of holdup are essential in the design of directional wells in order to effectively obtain practical pressure drop across the pipe and manage liquid amount transported [2]. Such design considerations affect hydrate formation, emulsion, wax deposition, and corrosion, all of which can impact flow assurance [3].

The strategy taken in order to estimate the liquid holdup can be summarized as identifying the boundary between the phases and labeling the area of each phase.

The initial step in processing the stratified wavy frames is to extract the annular section of the pipe by cropping the framing using minimum bounding box algorithm described in Chapter 2. The coordinates of the section to be cropped were manually specified based on observation and while cropping out the annular section was done for each frame, the procedure was made to take less time by using the same bounding box for each frame. This is valid because the camera and annular section locations did not change during video recording. The input and output images of this operation are shown in Figure 4.1.



(a)



(b)

Figure 4.1: Preprocessing of frames of stratified flow: (a) A frame as captured in the Stratified flow video (b) Annular region of frame extracted

Based on a comparison of the efficiency of using different thresholding algorithms on a set of selected frames, Otsu's technique for global thresholding that was mentioned in Chapter 2 was chosen to find a threshold that is used for boundary identification in the frames. The threshold was used in a Sobel filter, which determines edges as points of maximum gradient in the image. These maximum gradient points are determined by convolving the annular region image with a Sobel mask. This process also converts the frames in gray level to binary image.

In order to remove false edges and highlight the boundary between air and liquid phases, image opening – i.e. erosion followed by dilation – was performed on the resulting binary image. Different structuring elements (also called strels) were used in the dilation and erosion operations. The strels were chosen based on sampling of the effect of different strels of different shapes and sizes on many of the binary images with false edges.



Figure 4.2: Image of annular section with detected edges characterizing phase boundary.

The implemented opening operation also highlights the boundary by stretching the detected edges to fill the discontinuities between them. With the boundary between two phases now detected and highlighted, opposite sides of the boundary were labeled by setting all pixels on one side of the image that correspond to gas to a particular pixel value (255 was used), and the pixels on the other side of the boundary that correspond to water to another value (140 was used).

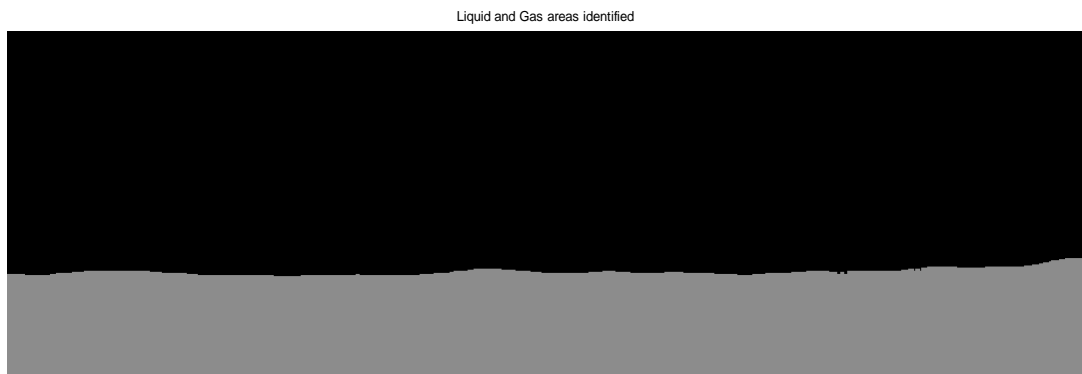


Figure 4.3: Flow image with gray and black labeling of liquid and gas areas respectively.

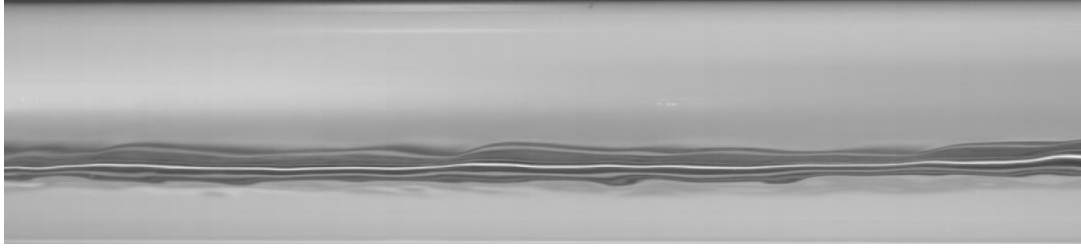
Having achieved an identification of areas of the image that correspond to liquid and gas phases, the liquid holdup value was estimated by:

Liquid holdup = total number of pixels in liquid area (pixels) / total number of pixels in
frame (pixels)

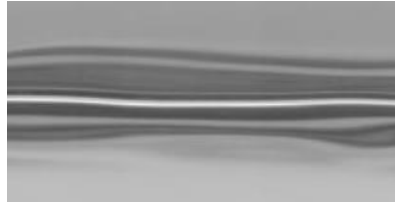
4.3 Estimation of Wave Celerity of Stratified flow

In Stratified wavy flow, the celerity of the interfacial wave is an indication of the multiphase flow velocity. The velocity of the fluid flowing in a pipe at any time is very important information for safe and optimal transportation through the pipe. In this work, an algorithm based on cross correlation of section of flow images is used to estimate wave celerity of stratified wavy flow. Some other approaches that have been used to solve the problem are described in Chapter 2.

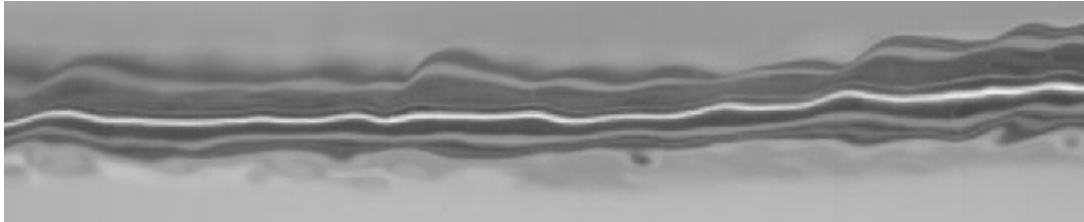
In a single run of the program, two consecutive frames from the recorded flow video are read into the program. Initial steps of annular section extraction by cropping are carried out on both images to obtain $f_1(x, y)$ and $f_2(x, y)$ respectively. A region, $r_1(x, y)$, located such that the waves are centrally located within it is cropped out of $f_1(x, y)$. A dimension of 207 x 163 was experimentally determined as being practically good enough for $r_1(x, y)$, with a consideration for operation speed, accuracy of results and the size of the frames in the recorded video, 1632 x 1200. The results of the cropping operation are shown in Figure 4.4.



(a)



(b)



(c)

Figure 4.4: Extracting flow wave: (a) An image of annular section, $f_1(x, y)$, from a frame of recorded stratified flow video. (b) $r_1(x, y)$, a centrally located region in $f_1(x, y)$ (c) An image of annular section, $f_2(x, y)$, from a frame of recorded stratified flow video.

In order to find the location of $r_1(x, y)$ in $f_2(x, y)$, a 2D normalized cross correlation of $r_1(x, y)$ and $f_2(x, y)$ was then carried out and Figure 4.5 shows a plot of a sample cross correlation matrix resulting from such operation. Normalizing the pixel values before the cross correlation operation yielded a faster overall operation than performing the cross

correlation without initially normalizing the pixel values. The indices of the element with the highest value in the resulting cross correlation matrix was then used to calculate the location of $r_1(x, y)$ in $f_2(x, y)$.

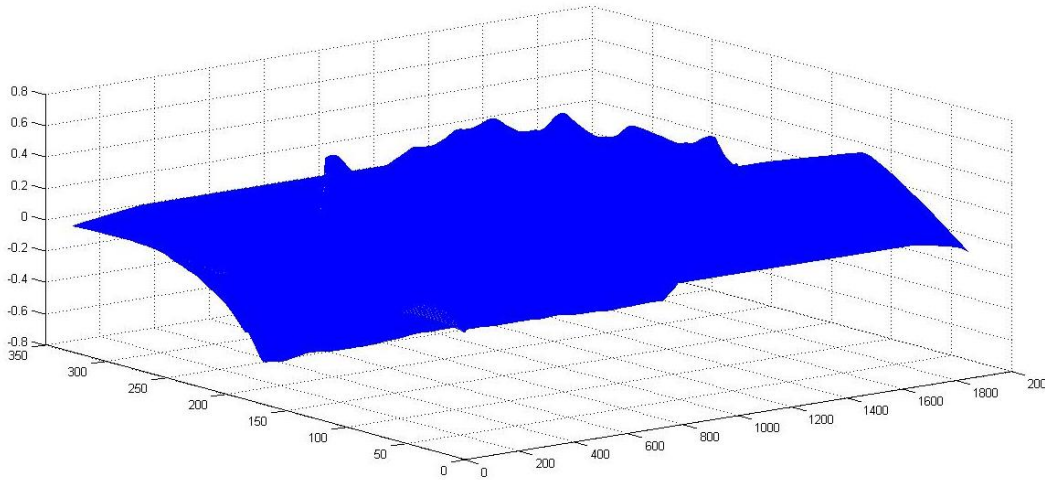


Figure 4.5: Plot of matrix of normalized cross correlation of $r_1(x, y)$ with $f_2(x, y)$

The difference in pixel coordinates of a corner in $r_1(x, y)$ and the same corner as located in $f_2(x, y)$ is calculated. The field of view of the camera is 0.1m and this corresponds to the 1632 horizontal pixels in each frame. The distance “moved” by the corner between $r_1(x, y)$ and $f_2(x, y)$ is then estimated using interpolation. The time interval between when the frames are captured is calculated from the video frame rate and wave celerity is then estimated by:

$$\text{Wave celerity} = \text{distance moved by corner (m)} / \text{time between frames (s)}.$$

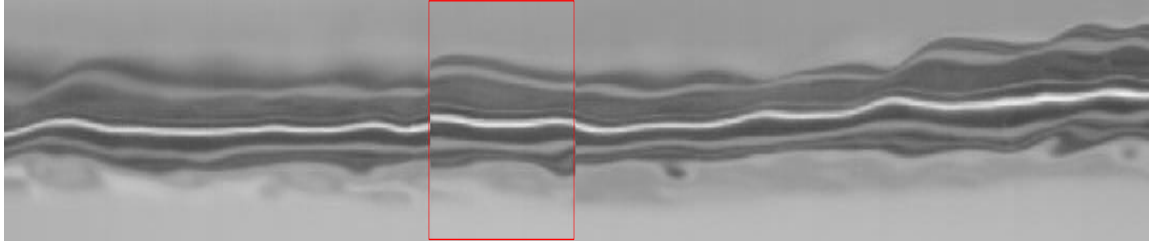


Figure 4.6: $f_2(x, y)$ with the location of $r_1(x, y)$, as estimated by the program, highlighted in a rectangle.

4.4 Estimation of Flow speed, Gas Volumetric Fraction & Average Gas speed of Bubbly flow

Estimating the properties of the gas phase in a multiphase flow is essential for optimal operation and monitoring of processes involving such flows. For example, properties of flows of wet gas in natural gas production change depending on reservoir conditions; and in order to ensure an efficient use of production resources, the amount of natural gas present in the flow from a reservoir is essential information. The speed of gas in multiphase flow transmission pipes is crucial in monitoring of the flow in order to maximize the pipe's throughput while ensuring the flow is not driving to slug or froth modes, which create unwanted stress on the pipes and other related equipment.

Due to increased activity in bubbly flow compared to stratified flow, there is a need for increased flow image preprocessing in the development of programs for the measurement of the above listed bubbly flow properties.

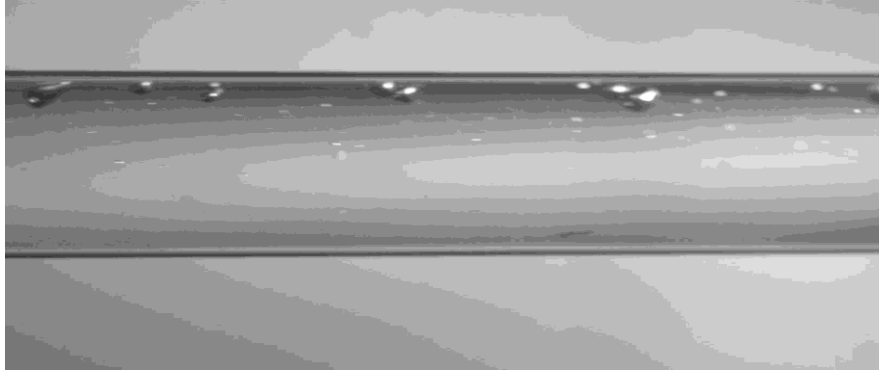


Figure 4.7: A sample bubbly flow image taken by the camera in the FVS used in this work (Grayscale, 8bits/pixel, 1200 x 1632).

4.4.1 Bubbly flow image preprocessing

The following are sequentially performed preprocessing operations that are performed on bubbly flow images used in estimating the properties of the flow

(i) Image cropping: In order to extract the annular section from an image frame from the bubbly flow video, minimum bounding box program was used to crop out the annular section from the image. Since the camera and pipe did not move throughout the flow recording, the bounding box dimensions that were determined to be suitable for one image of the flow sufficed for all the others.

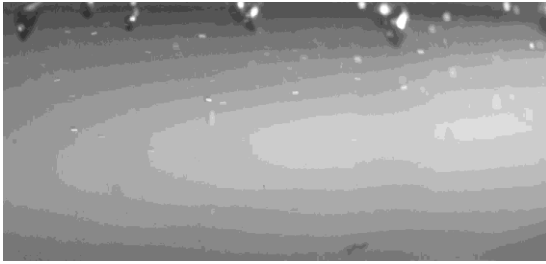
(ii) Illumination correction: While efforts were made to ensure appropriate illumination of all image objects in the flow recording, bubbles are often not evenly illuminated and some form of processing is necessary. To achieve uniform illumination of image objects, a top-hat filtering of the image is performed. Top-hat filtering is a kind of retrospective illumination correction method that involves morphologically opening the image with an appropriate structure element and subtracting the opened image from the original image. A sample result of this operation is shown in Figure 4.8(b).

(iii) Contrast adjustment: In order to properly account for image foreground objects, especially the medium and small bubbles, the contrast of the image was adjusted. A mapping of the intensity values in the illumination corrected image to new values such that 1% of the pixel values are 0 and another 1% are 255 was used to achieve this enhancement.

(iv) Image segmentation by global thresholding: Estimation of properties of gas phase in the flow is based on features of identified bubble objects. Before such identification can be carried out, edges of bubbles have to be detected. Image global thresholding by Otsu's method, which converts an intensity image to a binary image by using a threshold that minimizes the intraclass variance of the black and white pixels, was used. Figure 4.8 (d) is a sample result of this operation when performed on image in Figure 4.8 (c).

(v) Morphological opening: To ensure proper consideration of certain objects, we used area opening to remove noise and unwanted image objects. Opening is suitable because of the nature of the image objects that are regarded to as noise in the images. For example, to remove very small objects that occur in the image due to imperfect lighting but could be interpreted as tiny bubbles by the program, the image was opened to remove 8-neighborhood connected objects with a size of 50 pixels or less.

Figure 4.8 below shows the effect of each of these preprocessing operations in the order in which they are performed on the frame shown in Figure 4.7.



(a)



(b)



(c)



(d)



(e)

Figure 4.8: Bubbly image preprocessing. (a) Cropped gray level image to obtain annular section. (b) Annular section image with illumination correction. (c) Enhanced contrast annular section image (following illumination correction). (d) Segmented annular section image showing bubble objects (with noise). (e) Annular section image with bubble objects segmented and noise objects removed.

The high accuracy of bubble-segmentation of the overall preprocessing algorithm can be seen by visually comparing Figure 4.8 (a), a frame as obtained from a bubbly video, and Figure 4.8 (e), the resulting preprocessed image.

4.4.2 Estimation of properties of Bubbly flow from preprocessed images.

i) **Flow speed:** For the estimation of the speed of the multiphase flow, a program based on normalized cross correlation was developed. Two successive frames extracted from the flow video were cropped to extract their annular. A centrally located strip is then cropped from the first image. The strip is such that its height is equal to the height of the image of the annular section image (511 x 1632) so that it contains objects that correspond to small bubbles, big bubbles and the liquid phase. This strip is then correlated with the second frame using a normalized cross correlation algorithm and indices of the peak value in the resulting cross correlation matrix indicates the position of the strip in the second image. The pixel translation of the strip is calculated and the distance (in m) is interpolated from the knowledge of the FOV (0.1m) and pixel length (1632) of the annular sections. The flow speed is then estimated as:

$$\text{Flow speed} = \frac{\text{distance moved by corner of image strip between frames (m)}}{\text{time between frames (s)}}$$

ii) **Gas Volume fraction:** The ratio of the gas volumetric flow rate to the total volumetric flow rate of the multiphase fluid is called the gas volume fraction. In the developed program, it is estimated as the fraction of pixels associated with bubbles to the total pixels in the annular section. After all the preprocessing operations described in the subsection above were carried out, a program to find connected objects with an 8-connected neighborhood in the image and calculate the area and centroid of those objects was used to identify the bubbles in the image. With these values, the gas volume fraction was estimated as:

Gas volume fraction = number of pixels corresponding to bubbles (pixels) / number of pixels in annular section (pixels)

iii) **Average Gas speed:** The average gas speed is true speed (and not superficial speed) of the gas in the pipe section where the flow is recorded. While it changes across the pipe, it is a useful property of the flow especially at critical points in the transport line where stresses caused by the transported flow are highly undesirable.

In a bubbly flow consisting of large and small bubbles, the bubbles generally rise to the top of the pipe with an associated increase in size due to a drop in their density. Therefore, large bubbles are generally located close to the top of the pipe with small bubbles located in the mid region of the pipe. In the developed program, cross correlation involving a strip of the flow image taken from the top of the top section of the image was used to estimate the speed of the large bubbles and the cross correlation involving a strip from the middle section of the image is used to estimate the speed of the small bubbles. Using a threshold on the area property of identified bubbles, the bubbles were grouped into large and small bubbles. A pixel area value of 219 was found to be an appropriate threshold. The average gas speed for a given frame is then estimated as:

Average gas speed = (number of pixels corresponding to large bubbles/number of pixels in annular section) * speed of large bubbles + (number of pixels corresponding to small bubbles/number of pixels in annular section) * speed of small bubbles



(a)



(b)

Figure 4.9: Estimating average gas speed from processed bubbly flow images. (a) Processed image showing only big bubble objects (b) Processed image showing only small bubble objects

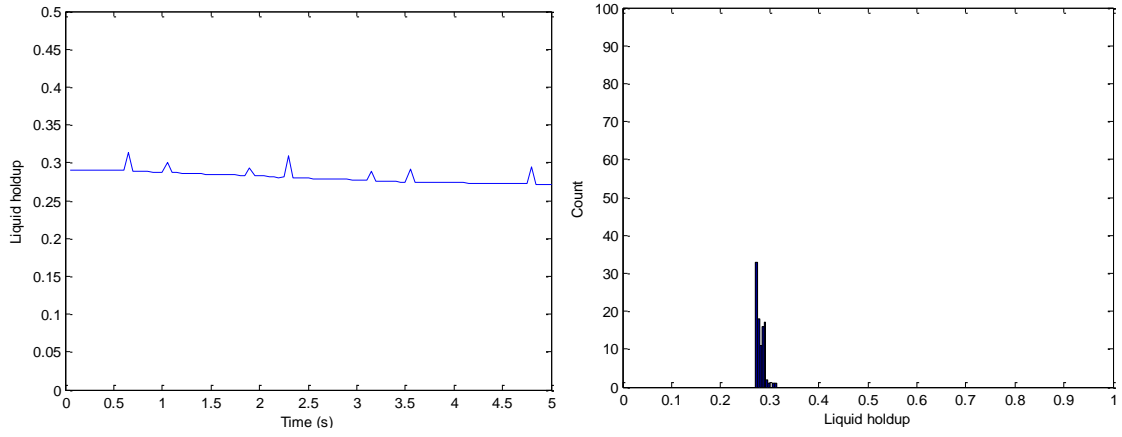
CHAPTER 5

DISCUSSION OF RESULTS

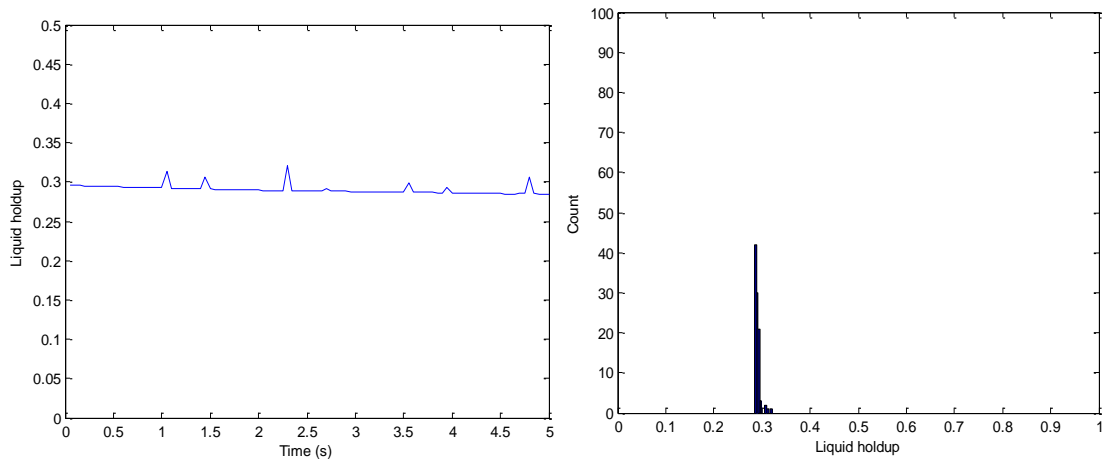
This section presents and discusses results from applying the programs described in the previous chapter to results from experiments described in Section 3.1.3. While flow videos were recorded for considerable periods in each experiment, the images used to obtain the results are those taken after 10 minutes from the commencement of the experiment. This is done to allow the experiment settle into its principal flow regime before taking images.

5.1 Liquid Holdup of Stratified flows

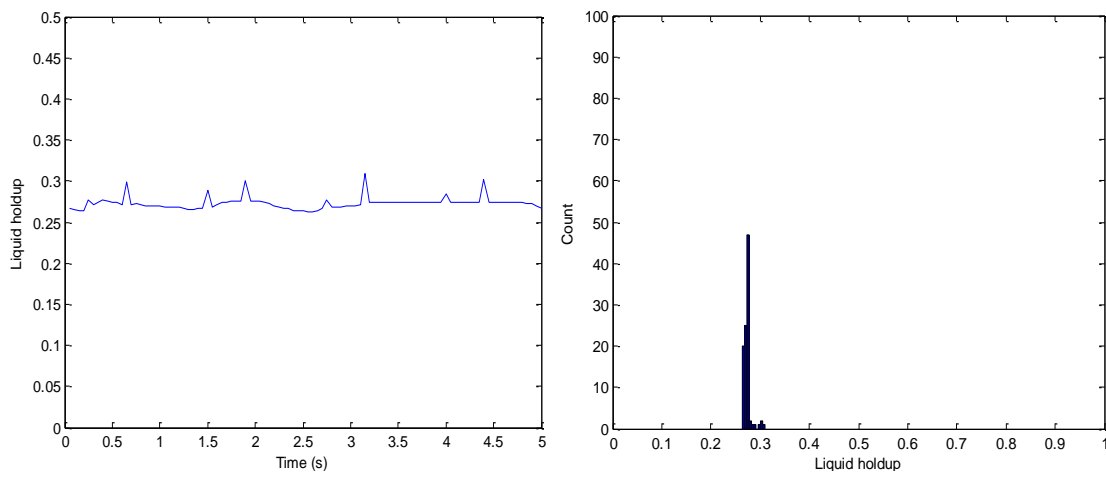
The liquid hold up of stratified flows of air and water obtained in the experiments were estimated using the video to frame conversion and hold up estimation programs described in Section 4.1. Figure 5.1 below shows the time series plot of the liquid holdup values for each experiment and a corresponding liquid holdup distribution plot.



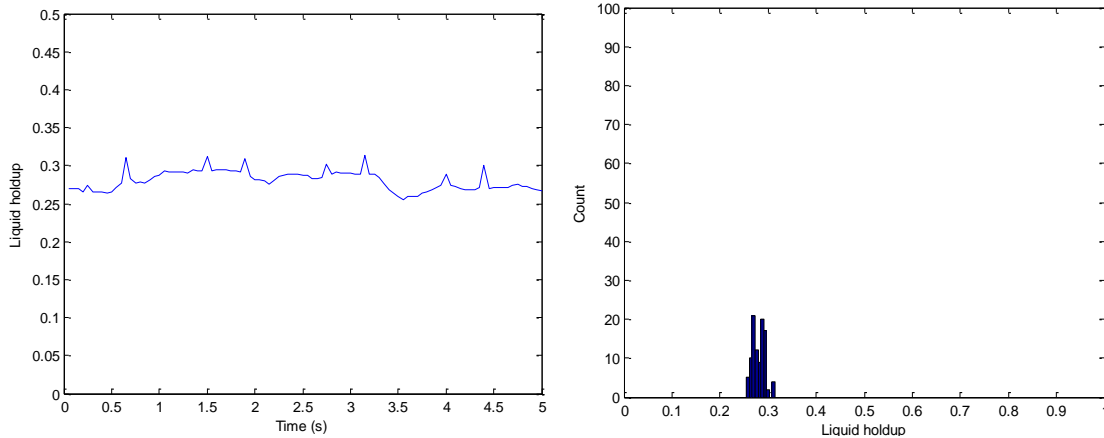
(a)



(b)



(c)



(d)

Figure 5.1: Time series plot and distribution plots of estimated liquid holdup for 5 seconds of stratified flows with (a) $V_{sg} = 0.2875$ m/s ; $V_{sl} = 0.33$ m/s (b) $V_{sg} = 0.3016$ m/s; $V_{sl} = 0.3317$ m/s (c) $V_{sg} = 0.3173$ m/s ; $V_{sl} = 0.33$ m/s (d) $V_{sg} = 0.3332$ m/s; $V_{sl} = 0.3317$ m/s.

Water cut is the proportion of water in a multiphase flow and Liquid holdup is the percentage of a section of flow that is occupied by liquid. Because of reduced activity in stratified flows, these values are typically equal [1]. The measured water cut in the experiment is 0.285 and the average estimated liquid in the four cases in Figure 5.1 are 0.2736, 0.2865, 0.2746 and 0.2848. These values are within ± 0.0114 (or 1.14%) of the measured value, indicating the accuracy of the developed algorithm.

In the time series graphs in Figure 5.1 (a) and (b), we see plots that are largely smooth. This indicates a largely smooth boundary between the liquid and gas phases in the flow and such flows are regarded to as stratified smooth flow.

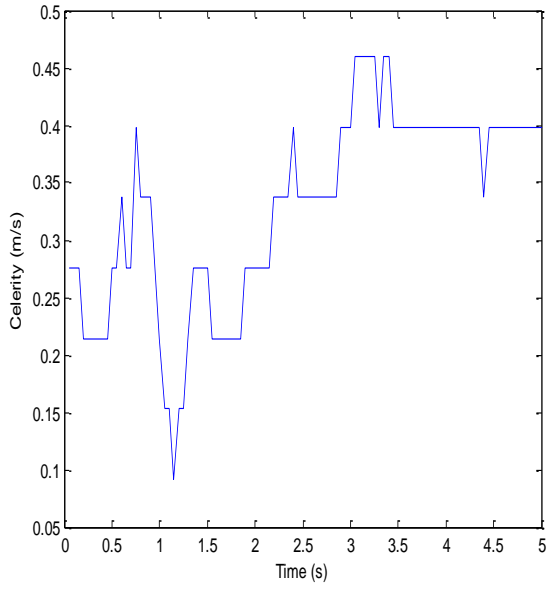
From the histogram plots, we see that the flows in Figure 5.1 (a) and (b) are also characterized by a liquid holdup value distribution plot whose values are gathered around a dominant value in a narrow range, indicating that there are very few variations of liquid

holdup in the considered period and location. Stratified smooth flow regimes occur in low superficial velocity flows with an absence of pressure fluctuations within the flow.

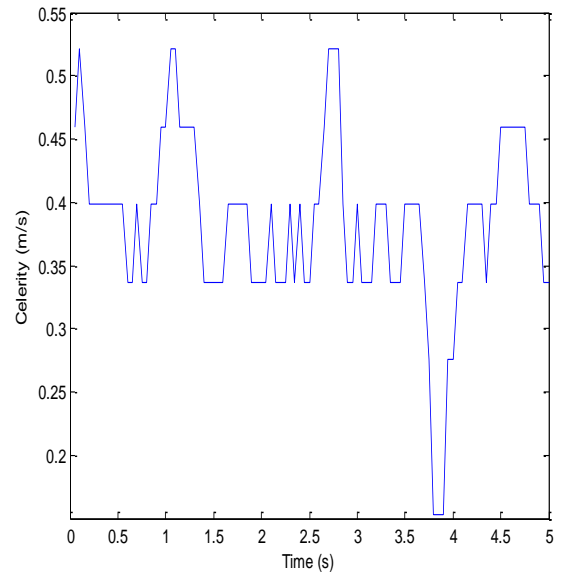
Compared with those in Figure 5.1 (a) and (b), the liquid holdup time series plot in Figure 5.1 (c) and (d) have a significantly wavy shape. This wave shape is indicative of the changing shape of the interfacial wave in the flow caused by the fluctuations of liquid holdup in the period considered. This is indicative of a Stratified wavy regime. The waves are initiated owing to the gas phase moving at a velocity that is sufficient to cause waves to form but lesser than that necessary for the initiation of a rapid wave that can cause a transition to intermittent or annular flow regimes. It can also be seen from the liquid holdup distribution plots that the liquid holdup values in stratified wavy flows spread over a slightly wider range – 0.0461 for Figure 5.1 (c) and 0.0588 for Figure 5.1 (d) – when compared with stratified smooth flows – 0.0401 for Figure 5.1 (a) and 0.0359 for Figure 5.1 (b).

The plots are of values obtained from processing frames from a 5s section of the flow videos. Similar plots in regular intervals can be used to monitor the wetness of a multiphase flow such as in monitoring the amount of liquid contained in the output of a normally dry gas field [10], which is essential information in optimizing reservoir output.

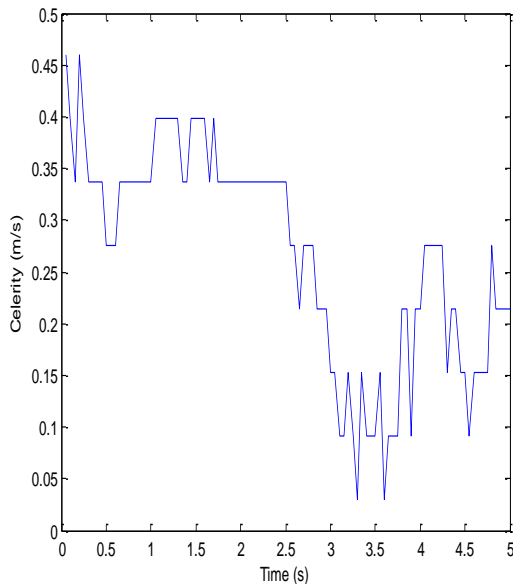
5.2 Wave celerity of Stratified flows



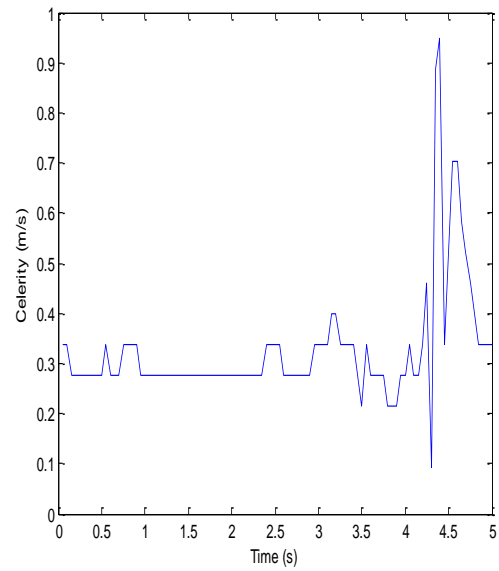
(a)



(b)



(c)



(d)

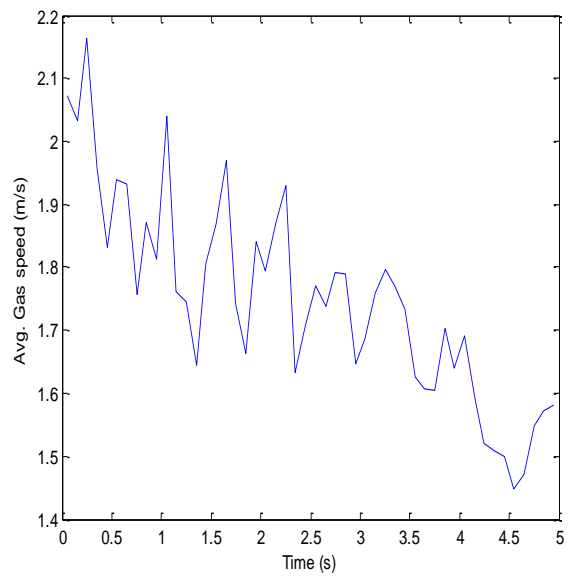
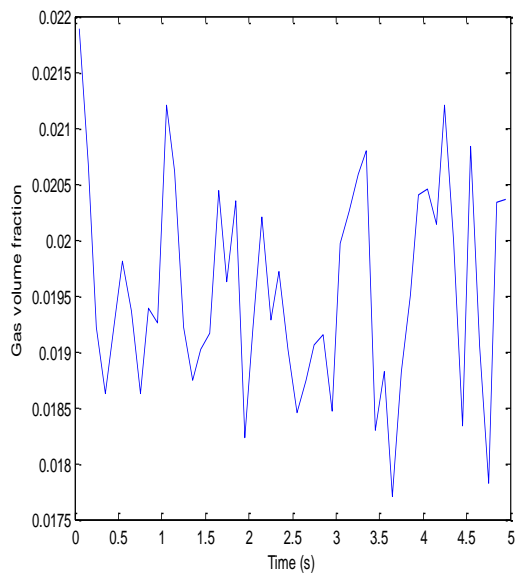
Figure 5.2: Time series plot of estimated wave celerity through frames for 5 seconds of stratified flows with (a) $V_{sg} = 0.2875$ m/s ; $V_{sl} = 0.33$ m/s (b) $V_{sg} = 0.3016$ m/s; $V_{sl} = 0.3317$ m/s (c) $V_{sg} = 0.3173$ m/s ; $V_{sl} = 0.33$ m/s (d) $V_{sg} = 0.3332$ m/s; $V_{sl} = 0.3317$ m/s.

Compared with liquid holdup plots, the wave celerity plots in Figure 5.2 are less smooth. This is because the activity at the boundary between the phases, which is where the wave is located and estimated, is much more influenced by properties of both phases. Generally, the wave celerity only gets or stays higher than the gas phase velocity because the celerity is a resultant of both gas and liquid phase velocities. If a sustained wave celerity value that is higher observation is noticed in the time series plot, one reason could be an increase in superficial velocity of the one or both constituent phases.

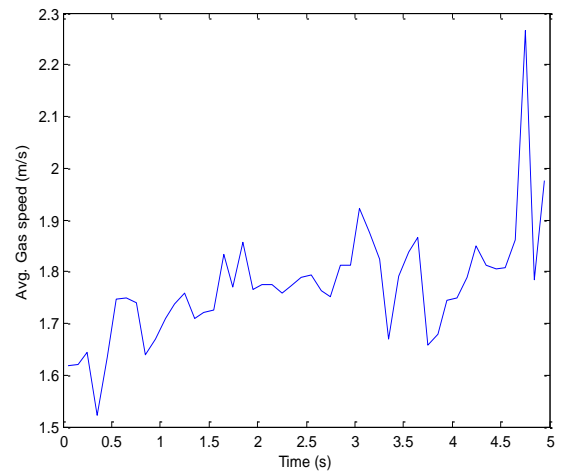
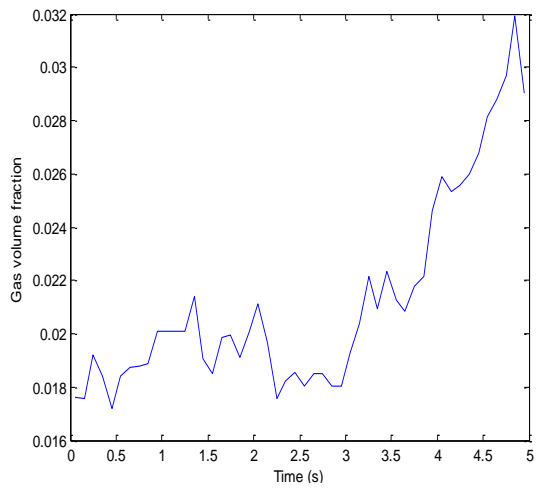
Similar plots of values obtained from periodically processing a number of frames of the flow in can be used to monitor the speed of propagation of the waves of a multiphase flow, which can be used as an indication of the stress the flow could be cause to surrounding equipment that are transporting the multiphase flow.

5.3 Gas Volume Fraction and Average Gas speed of Bubbly flows

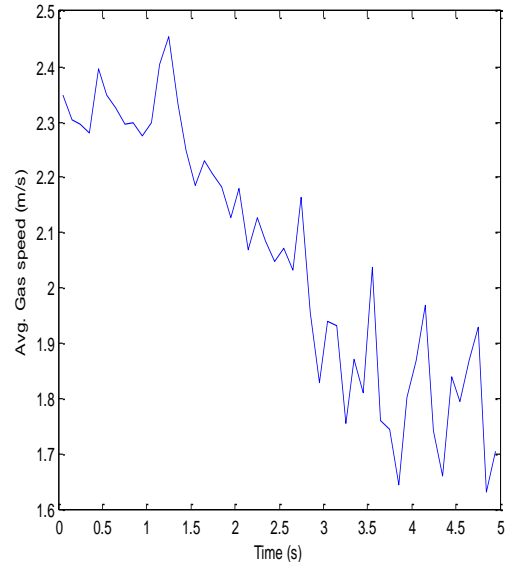
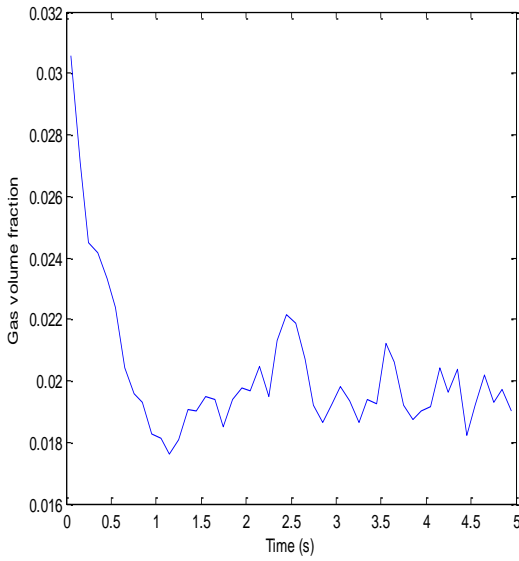
Wet gas is a term used to define a variety of gas conditions, ranging from gas that is saturated with liquid vapor to a multiphase flow with a 90% volume of gas. Because of the effect of varying densities of its constituent fluids, characterizing a wet gas is of particular significance in industrial multiphase flow measurement. Figure 5.3 below shows the gas volume fraction and average gas speed as estimated from videos of 4 cases of bubbly flow regimes.



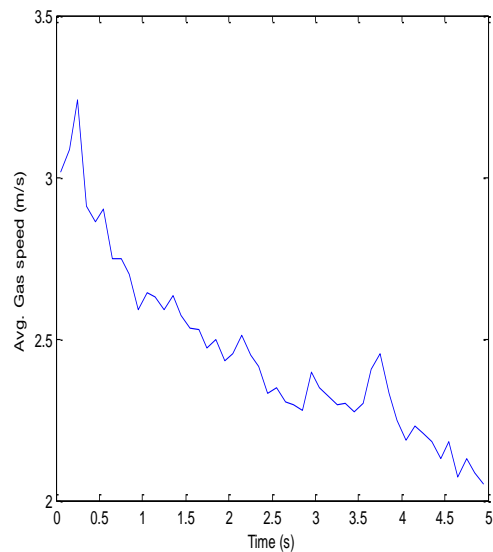
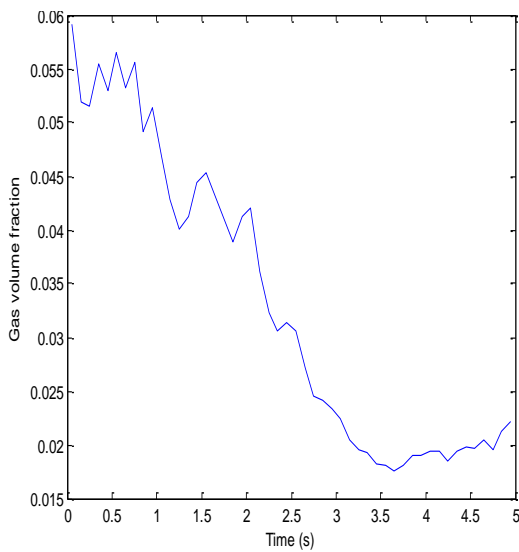
(a)



(b)



(c)



(d)

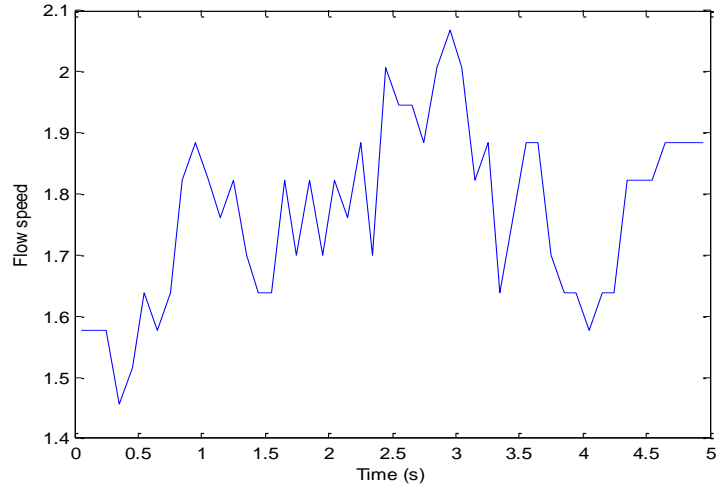
Figure 5.3: Time series plots of estimated gas volume fraction and average gas speed for 5 seconds of bubbly flows with (a) $V_{sg} = 0.3173$ m/s ; $V_{sl} = 0.3316$ m/s (b) $V_{sg} = 0.3649$ m/s ; $V_{sl} = 0.3332$ m/s (c) $V_{sg} = 0.8410$ m/s ; $V_{sl} = 0.3316$ m/s (d) $V_{sg} = 1.1106$ m/s ; $V_{sl} = 0.3332$ m/s

Volumetric fraction and phase velocity are the most important properties measured in multiphase flows. In gas-focused processes industrial processes, gas volume fraction and

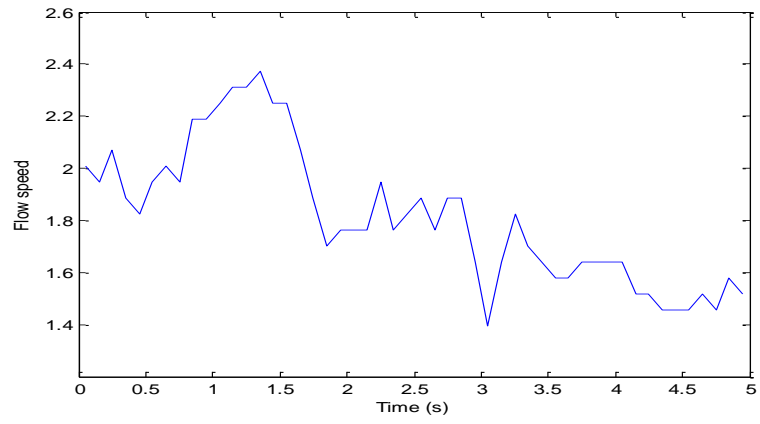
average gas speed readings become even more important. It can be observed from the plots that the average gas speed of the multiphase flow increases with an increase in superficial velocity of the gas phase – at $V_{sg} = 0.3173$ m/s; maximum average gas speed in the flow is 2.153 m/s and at $V_{sg} = 1.1106$ m/s, maximum average gas speed in the flow is 3.251 m/s. The gas volume fraction also follows the same trend and this is consistent with what is known of gas flows. While gas properties in a multiphase flow tend to change rapidly because of the constant flux in properties of the flow such as its pressure and dispersion, the high frequency of measurement – 1000 readings per second - makes the plots appear extra erratic.

5.4 Flow speed of Bubbly flows

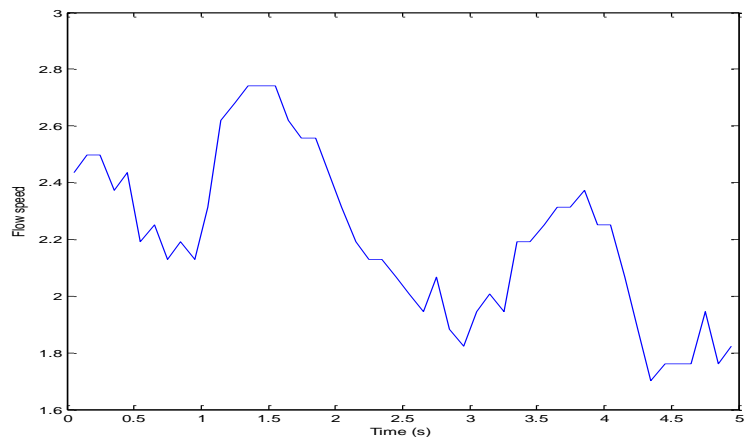
Measurement of the rate of flow is the quintessential use of all flow metering devices. While measuring the properties of individual phases in a multiphase flow is a requirement of multiphase flow meters, measuring the rate of the overall multiphase flow is still necessary. The plots below present the overall flow speed (in m/s) of recorded bubbly flows over 5s.



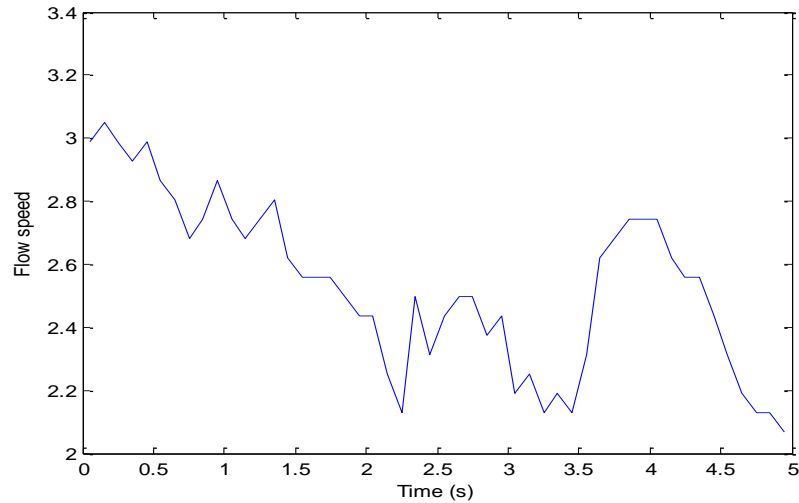
(a)



(b)



(c)



(d)

Figure 5.4: Time series plots of flow speed for 5 seconds of bubbly flows with (a) $V_{sg} = 0.3173$ m/s ; $V_{sl} = 0.3316$ m/s (b) $V_{sg} = 0.3649$ m/s; $V_{sl} = 0.3332$ m/s (c) $V_{sg} = 0.8410$ m/s ; $V_{sl} = 0.3316$ m/s (d) $V_{sg} = 1.1106$ m/s; $V_{sl} = 0.3332$ m/s.

As with average gas speed, the maximum speed of the multiphase flow increases with an increase in gas superficial velocity – at $V_{sg} = 0.3173$ m/s, maximum average gas speed in the flow is 2.083 m/s and at $V_{sg} = 1.1106$ m/s, maximum average gas speed in the flow is 3.091 m/s. However, the overall flow speed is generally slightly lesser than the average gas speed. This can be explained as owing to the reverse or recirculating motion of a part of the liquid phase [1].

5.5 Analysis of the developed programs

While the results of this work contribute to theoretical research into multiphase flow, we were more concerned with the potential for practical use of the developed system of multiphase flow measurement. In this regard, it is important to consider the speed and

resource usage of the software in an image processing system for multiphase flow measurement.

In this work, five programs to estimate five flow properties – Liquid holdup and wave celerity of Stratified flows and Average gas speed, Gas volume fraction and Flow speed of bubbly flows – were developed. As described in Chapter 4, Video to image and image preprocessing programs are invoked during the execution of each of these programs. All programs are implemented using MATLAB R2013b on a HP Pavilion 15-P073TX PC with Intel Dual Core i7 2.00 GHz 2.60 GHz 64-bit CPU, 8.00GB RAM and 1 TB HDD memory. Table 5.1 below shows the average execution time during their execution to estimate flow properties from 5s (which is equivalent to 5000 images) of flow videos that are presented in previous sections.

Table 5.1: Average run time of developed programs

| Program to estimate... | Average execution time (s) |
|------------------------------------|----------------------------|
| Liquid holdup in Stratified flow | 2.751 |
| Wave celerity in Stratified flow | 28.250 |
| Average Gas speed in Bubbly flow | 51.126 |
| Gas volume fraction in Bubbly flow | 3.011 |
| Flow speed in Bubbly flow | 37.332 |

The major reason why some of the programs have run time that is far greater than others is the normalized cross correlation operation. The programs for holdup in stratified flow and Gas volume fraction in bubbly flow do not involve cross correlation and as such have reduced times. The program for the estimation average gas speed in bubbly flow involves two normalized cross correlation operations; one for large bubbles and another for small bubbles.

Although efforts such as normalizing the values to be cross correlated were made to optimize the programs, it can be seen from Table 5.1 that for most of the programs, a deployment for real time application will not be feasible with the developed programs. However, leveraging parallel processing and high power computing technologies is an interesting prospect in addressing this challenge.

CHAPTER 6

RECOMMENDATIONS AND CONCLUSION

6.1 Recommendations for future work

This work contributes to the research into the use of image processing paradigms in multiphase flow measurement by developing programs that are to multiphase flow videos to estimate flow properties and implementing a model test section that can be a basis for further research. Although decent results were obtained from our efforts, the following are recommendations that could lead to a more accurate and generalized system.

- Subjectivity is a substantial feature of image processing algorithms. Although we tried to make the developed algorithms requiring as little human interaction (in the form of parameter entry) as possible, subjective parts of the developed algorithms such as dimensions for cropping the annular section of images of different flows and validating estimated threshold used in edge detection subroutines would be significant improvements.
- Executing the programs using parallel processing and high performance computing technology to increase the speed of execution and amount of data obtained. This could generally make the system suitable for practical use in sensitive areas.

- While 2 phase flows are quite common in the process industry, extending the ideas in this work to flows with more than 2 phases – such as flows of oil, water and air – will be of significant use.
- The patent in [15], which was co-authored by members of the thesis committee, was a source of some of the ideas implemented in this work and contains other novel ideas – such as using images from 2 cameras mounted along the flow in order to use 3-D flow visualizations (instead of 2-D) in the programs – that could make the system more robust if implemented.

6.2 Conclusion

Based on the research, experimental work and program development carried out in this work, the following are conclusions that were reached:

- From discussion of the obtained results, using image processing techniques in multiphase flow measurement offer a real potential in obtain usable flow measurements.
- While real time application could not be achieved in this work, the run time of the developed algorithms indicate the feasibility of achieving real time implementation of algorithms with similar applications.
- There are few works that have considered the practical use of image processing systems and techniques for flow measurement. However, the resourcefulness that comes from being able to use one setup for many kinds of flow regimes and the continuing rapid growth in image processing technology amongst other factors

makes the use of image processing in multiphase flow measurement of substantial interest.

References

- [1] S. Levy, “Two-Phase Flow in Complex Systems,” *Wiley Publishing*. 1999
- [2] C.D. Han, “Multiphase Flow in Polymer Processing,” *Academic Press*, 1981.
- [3] R. E. Guzman and F.J Fayers, “Mathematical Properties of Three-Phase Flow Equations,” *Society of Petroleum Engineers*, doi:10.2118/35154-PA, 1997.
- [4] “Thermopedia: A-Z Guide to Thermodynamics, Heat & Mass Transfer and Fluids Engineering.” *Semantic Globe*, 2014
- [5] T. Shea. “Multi-phase flow metering gains acceptance in upstream applications.” *ARC Advisory Group, Offshore-mag.com*, 2013
- [6] G. Falcone, G.F. Hewitt and C. Alimonti. “Multiphase Flow Metering– Principles and Applications.” *Developments in Petroleum Science*, Vol. 54, Elsevier, Amsterdam. 2010.
- [7] “Weatherford Alpha VSRD Multiphase Flowmeter Brochure.” *Weatherford*. 2010
- [8] “State of the art multiphase flow metering,” *American Petroleum Institute*. 2004
- [9] R.Thorn, G.A. Johansen and E.A. Hammer, “Three-Phase Flow Measurement in the Offshore Oil Industry: Is there a place for Process Tomography” *1st World Congress on Industrial Process Tomography*, Buxton, Greater Manchester. 1999
- [10] “Guidance Notes for Petroleum Measurement. Issue 9.1” *Department of Energy & Climate Change*, UK. 2015
- [11] S. Mack and J. William, “Steady-State Multiphase Flow- Past, Present, and Future, with a Perspective on Flow Assurance,” *Energy Fuels*, Vol. 26, No.7, pp 4145–4157. 2012.
- [12] “See what GE is doing in Bangalore, Shanghai, and New York to innovate on oil and gas technology,” *Quartz*, India. 2005

- [13] M. Kumar, "Multiphase Flow Metering: An Overview," *General Electric*. 2013
- [14] B. G. Pinguet, "Worldwide Review of 10 years of the Multiphase Meter Performance Based on a Combined Nucleonic Fraction Meter and Venturi in Heavy Oil," *29th International North Sea Flow Measurement Workshop*, October, 2011.
- [15] M. Elshafei, F. Al-Sunni, and S. El-Ferik, "Multi-phase flow identification and measurement using image correlation," *Patent US US20130211746 A1*. 2013.
- [16] C.T. Crowe Taylor and F.B. Raton, "Multiphase Flow Handbook," 2006.
- [17] W.F.J Slijkerman, A.W. Jamieson, W.J. Priddy, O. Oakland, and H. Moestue, "Oil companies' needs in multiphase flow metering," *Proc. 13th North Sea Flow Measurement Workshop*. Norway. 1995
- [18] A. Richards, "Downhole multiphase metering," *Proc. Conf. on the Future of Multiphase Metering* 1998
- [19] E.A. Hammer and J.E. Nordtvedt, "The application of a Venturi meter to multiphase flow meters for oil well production," *Proc. 5th Conf. Sensors and Applications*, London, 1991.
- [20] R. Thorn, G.A. Johansend and E.A. Hammer, "Recent Developments in Three-Phase Flow Measurement," *Measurement Science Technology*. pp 691-701. 1997
- [21] "Safire 2.0 datasheet" *General Electric Company*. 2015
- [22] H. Mohamed, T. Adrien, D. Younes, and A. Jean-Francois, "Virtual Flow Meter Pilot: Based on Data Validation and Reconciliation Approach," *SPE international Production and Operation Conference and Exhibition*, Doha Qatar. 2012.
- [23] O. Bratland "Pipe Flow Multiphase flow assurance Book." 2009.
- [24] O. Bratland. "Update on Commercially Available Flow Assurance Software Tools: What they can and cannot do?" *4th Asian Pipeline Conference & Exhibition*. Kuala Lumpur 2008

- [25] M. Honkanen, H. Eloranta and P. Saarenrinne. “Digital imaging measurement of dense multiphase flows in industrial processes,” *Flow Measurement and Instrumentation*, vol. 21, pp. 25-32. 2010.
- [26] T. Bui-Dinh and T.S. Choi, “Application of image processing techniques in air/water two phase flow,” *Mechanics Research Communications*, Vol.26, No.4, pp. 463–468. 1999.
- [27] D. Amaral, R.F. Alves, M.J. da Silva, L.V.R. Arruda, L. Dorini, R.E.M. Morales, and D.R. Pipa, “Image processing techniques for high-speed videometry in horizontal two-phase slug flows,” *Flow Measurement and Instrumentation*, Vol.33, pp. 257–264. 2013.
- [28] A. Murat, and H. Ertan, “Analysis of gas–liquid behavior in eccentric horizontal annuli with image processing and artificial intelligence techniques,” *Journal of Petroleum Science and Engineering*, Vol. 81, pp. 31–40. 2012.
- [29] A. Zarubaa, E. Kreppera, H.M. Prassera, and B.N. Reddy, “Experimental study on bubble motion in a rectangular bubble column using high-speed video observations,” *Flow Measurement and Instrumentation*, Vol.16, No. 5, pp. 277–287. 2005.
- [30] Point Grey Research. “Machine Vision Interface Comparison and Evolution,” 2015.
- [31] R.C. Gonzalez, R.E. Woods and L.E. Steven “Digital Image Processing Using MATLAB, 2nd ed.,” *Gatesmarks publishing*, 2009.
- [32] Z. Karel, “Contrast Limited Adaptive Histogram Equalization” *In Graphics Gems IV*, Academic Press Professional, Inc. pp. 474-485. San Diego, CA, USA: 1994.
- [33] C. John “The image processing handbook, Fifth edition,” *CRC Press*, 2006.
- [34] X. Zhu, “The Application of Wavelet Transform in Digital Image Processing.” *International Conference on Multi Media and Information Technology. MMIT '08. Three Gorges*, pp. 326 – 329. 2008.

- [35] D. Wang, T. Dillon, and E. Chang, "Pattern learning based image restoration using neural networks". *Conference: Proceedings of the International Joint Conference on Neural Networks, IJCNN '02*. Volume 2. 2002
- [36] F. Qiu, Y Wang, M Jiang, and D Yuan., "Adaptive Image Restoration Based on the Genetic Algorithm and Kalman Filtering". *Advanced Intelligent Computing Theories and Applications. With Aspects of Contemporary Intelligent Computing Techniques*. '07. Volume 2 pp. 742-750, 2007
- [37] N. Li and Y. Li, "Image Restoration using Improved Particle Swarm Optimization," *International Conference on Network Computing and Information Security*. 2011
- [38] "WOLFARM," Language and System, Documentation center. <http://reference.wolfram.com/language/ref/Inpaint.html>. 2015
- [39] "Oilfield Glossary." Schlumberger Limited. 2015
- [40] A. Bonilla, A.C. Bannwart, and O.M.H. Rodriguez, "Holdup estimation in core flow using image processing," *Instrumentation and Measurement Technology Conference*. Campinas, Brazil. 2013
- [41] J. Mohsen, "Particle Image Velocimetry: Fundamentals and Its Applications" *Göteborg Research*, Chalmers University of Technology. 2011.
- [42] A.M. Ozbayoglu and H.E. Yuksel, "Analysis of gas-liquid behavior in eccentric horizontal annuli with image processing and artificial intelligence techniques," *Journal of Petroleum Science and Engineering* Elsevier. 2012
- [43] A. Jaworek, A. Krupa and M. Trela, "Capacitance sensor for void fraction measurement in water/steam flows," *Flow Measurement and Instrumentation*, vol. 15, pp. 317-324, October-December 2004.
- [44] U. Hampel, J. Otahal, S. Boden, M. Beyer, E. Schleicher, W. Zimmermann, and M. Jicha, "Miniature conductivity wire-mesh sensor for gas-liquid two-phase flow

- measurement,” *Flow Measurement and Instrumentation*, vol. 20, pp. 15-21, March 2009.
- [45] Deendarlianto A. Ousaka, A. Kariyasaki and T. Fukano, “Investigation of liquid film behavior at the onset of flooding during adiabatic countercurrent air–water two-phase flow in an inclined pipe,” *Nuclear Engineering and Design*, vol. 235, pp. 2281-2294, October 2005.
- [46] Y. Murai, Y. Tasaka, Y. Nambu, Y. Takeda and S.R. Gonzales, “Ultrasonic detection of moving interfaces in gas–liquid two-phase flow,” *Flow Measurement and Instrumentation*, vol. 21, pp. 356-366, September 2010.
- [47] H.C. Yang, D.K. Kim and M.H. Kim, “Void fraction measurement using impedance method,” *Flow Measurement and Instrumentation*, vol. 14, pp. 151-160, August-October 2003.
- [48] M. Banowski, D. Lucas and L. Szalinski, “A new algorithm for segmentation of ultrafast X-ray tomographed gas–liquid flows,” *International Journal of Thermal Sciences*, vol. 90, pp. 311-322, April 2015.
- [48] Ayinde, Babajide O. and Ahmed H. Desoky. "Lossless Image Compression using Zipper Transformation." In International Conference on Image Processing, Computer Vision & Pattern Recognition, Las Vegas. July, 2016.
- [49] P. Stahl and P.R. von Rohr, “On the accuracy of void fraction measurements by single-beam gamma-densitometry for gas–liquid twophase flows in pipes,” *Experimental Thermal and Fluid Science*, vol. 28, pp. 533-544, June 2004.
- [50] Y. Han, N. Shikazono and N. Kasagi, “Measurement of liquid film thickness in a micro parallel channel with interferometer and laser focus displacement meter,” *International Journal of Multiphase Flow*, vol. 37, pp. 36-45, January 2011.
- [51] S. Becker, H. De Bie, and J. Sweeney, “Dynamic flow behaviour in bubble columns,” *Pergamon Chemical Engineering Science* 54. pp 4929-4935. 1999

- [52] J.J. Xiao, O. Shoham, and J.P. Brill, "A comprehensive Mechanistic Model for Two-phase flow in pipelines" *SPE Annual Technical conference and Exhibition*. 1990
- [53] El-Sebakhy and A. Emad, "Flow regimes identification and liquid-holdup prediction in horizontal multiphase flow based on neuro-fuzzy inference systems," *Mathematics and Computers in Simulation*, Vol. 80 Issue 9, May 2010.
- [54] K. Nishino, H. Kato, and K. Torii, "Stereo Imaging for simultaneous measurement of size and velocity of particles in dispersed two-phase flow". *Measurement Science and Technology* . pp 633-645. 2000
- [55] D. Burkle, T. Preusser, M. Rumpf. "Transport and anisotropic diffusion in time-dependent flow visualization". *Proceedings of the IEEE Visualization Conference*, San Diego, CA, Oct 21–26 2001, pp. 61–67.
- [56] O. Melander, "Fluid dynamics and flow structures of wood fibres suspended in gas flows", *Doktorsavhandlingar vid Chalmers Tekniska Hogskola*, 2415, 1–68. 2006.
- [57] S. Goto, Y. Ishizaki, H. Ohashi, and M. Akiyama, "Characteristic behavior of bubbles and slugs in transient two-phase flow using image-processing method." *Trans. Jpn. Soc. Mech. Eng. B* 61 (585), 1626–1631. 2006
- [58] M. Gopal ,W.P Jepson. "Development of digital image analysis techniques for the study of velocity and void profiles in slug flow". *Int. J. Multiph. Flow* 2 (5), 945–965 Sep 1997.
- [59] T. Miyahara, M. Hamaguchi, Y. Sukeda, and T. Takahashi, "Size of bubbles and liquid circulation in a bubble column with a draught tube and a sieve plate." *Canadian Journal of Chemical Engineering* 64, 717-725. 1986
- [60] J.H.J. Kluytmans, B.G.M. Van Wachem, B.F.M Kuster, R. Krishna, and J.C. Schouten, "Image Analysis to Quantify Sizes, Velocities, Interfacial Areas, and

Coalescence Behavior of Gas Bubbles in a 2D Bubble Column”. *Measurement Science and Technology*, Chapter 2. 2002

- [61] D. Cheng, H. Burkhardt. “Template-based bubble identification and tracking in image sequences,” *International Journal of Thermal Science* 45, 321-330. 2006
- [62] W.R. Oliveira, I.B. de Paula, F.J.W.A. Martins, P.S.C. Farias, and L.F.A. Azevedo, “Bubble characterization in horizontal air – water intermittent flow” *Int. J. of Multiphase Flow*. Vol 69 pp 18-30. 2015.
- [63] H.Y. Kuntoro, A.Z. Hudaya, O. Dinaryanto, Deendarlianto, and Indarto., “Experimental Study of the Interfacial Waves in Horizontal Stratified Gas-liquid Two-phase Flows by Using the Developed Image Processing Technique” *International Forum on Strategic Technology*. 2015
- [64] M. Al-Nasser. “Multiphase Flow estimation using Image Processing (Dissertation Proposal)” *Department of Systems Engineering, KFUPM*. 2014
- [64] Ayinde, Babajide O., Ehsan Hosseini-Asl, and Jacek M. Zurada. "Visualizing and Understanding Nonnegativity Constrained Sparse Autoencoder in Deep Learning." *International Conference on Artificial Intelligence and Soft Computing*, pp. 3-14. Springer International Publishing, 2016.
- [65] Ayinde, Babajide Odunitan, and Abdulaziz Y. Barnawi. "Differential evolution based deployment of wireless sensor networks." *Computer Systems and Applications (AICCSA), 2014 IEEE/ACS 11th International Conference on*, pp. 31-137. IEEE, 2014.
- [66] Hashim, Hashim A., B. O. Ayinde, and M. A. Abido. "Optimal placement of relay nodes in wireless sensor network using artificial bee colony algorithm." *Journal of Network and Computer Applications* 64 pp: 239-248. 2015
- [67] Ayinde, Babajide O., Sami El Ferik, Salim Ibrir, Moez Feki, and Bilal A. Siddiqui. "Backstepping control of an electro-hydraulic servo system subject to

disturbance and parameter uncertainty." *GCC Conference and Exhibition (GCCCE), 2015 IEEE 8th*, pp. 1-6. IEEE, 2015.

[68] Ferik, Sami El, Babajide Odunitan Ayinde, Salim Ibrir, and Moez Feki. "Backstepping-based output feedback control of an electro-hydraulic servo system." *Systems, Signals & Devices (SSD), 2015 12th International Multi-Conference on*, pp. 1-6. IEEE, 2015.

[69] Ayinde, Babajide O. and J. M. Zurada. "Clustering of Receptive Fields in Autoencoder." *International Joint Conference on Neural Networks*, Vancouver. IEEE, May, 2016.

|

Vitae

Name :Abubakar, Shamsudeen Olawale |

Nationality :Nigerian |

Date of Birth :6/5/1990|

Email :abus155@yahoo.com|

Education

- BSc. Computer Engineering, 2011. University of Lagos, Lagos, Nigeria.
- MSc. Systems and Control Engineering, 2016. King Fahd University of Petroleum and Minerals, Saudi Arabia.